Recent Advances in Resonant Waveguide Gratings

*Giorgio Quaranta, Guillaume Basset, Olivier J. F. Martin, and Benjamin Gallinet**

Resonant waveguide gratings (RWGs), also known as guided mode resonant (GMR) gratings or waveguide-mode resonant gratings, are dielectric structures where these resonant diffractive elements benefit from lateral leaky guided modes from UV to microwave frequencies in many different configurations. A broad range of optical effects are obtained using RWGs such as waveguide coupling, filtering, focusing, field enhancement and nonlinear effects, magneto-optical Kerr effect, or electromagnetically induced transparency. Thanks to their high degree of optical tunability (wavelength, phase, polarization, intensity) and the variety of fabrication processes and materials available, RWGs have been implemented in a broad scope of applications in research and industry: refractive index and fluorescence biosensors, solar cells and photodetectors, signal processing, polarizers and wave plates, spectrometers, active tunable filters, mirrors for lasers and optical security features. The aim of this review is to discuss the latest developments in the field including numerical modeling, manufacturing, the physics, and applications of RWGs. Scientists and engineers interested in using RWGs for their application will also find links to the standard tools and references in modeling and fabrication according to their needs.

1. Introduction

1.1. From Diffraction Gratings to Resonant Waveguide Gratings

Wood's observation of rapid variations in the reflected diffraction orders from ruled gratings have prompted an extensive amount of research:[1] Rayleigh gave the first interpretation of part of those anomalies 5 years later in terms of appearance or disappearance of diffracted orders from or into evanescent modes, respectively.[2] In 1941, Fano proposed that some anomalies may be created by the excitation of surface waves on the grating surface.[3] Hessel and Oliner employed an original theoretical approach based on guided waves rather than on scattering and could explain anomalies of deep grating groove geometries using numerical tools, corroborating the explanation proposed by Fano.[4] Maystre developed in 1972 a rigorous vector theory able to accurately compute the properties of metallic gratings with any profile for any wavelength.[5] Experimental results used along this investigation exhibited variations associated with the metal used for the grating or the manufacturing method—especially with the presence of a metal oxide layer or a dielectric coating on the metal grating—thus supporting the existence of leaky guided surface waves with variable intensities. Later, such gratings supporting quasi-guided modes have been referred to as resonant waveguide gratings (RWGs) and are also known as guided mode resonant (GMR) gratings or devices, leaky mode resonant gratings, grating slab waveguides, resonant diffraction gratings, (resonant) grating waveguide structures, resonant subwavelength gratings(SWGs), resonance grating couplers, or waveguide-mode resonances (WMRs). Cross-section examples of RWGs are shown in **Figure 1**. They differ from high contrast gratings (HCGs), in which there are multiple vertical Bloch modes between the upper and lower grating boundaries.[6] The main difference is that RWGs rely on resonances with waves propagating along the grating, the so-called leaky modes. In HCGs, there are also leaky modes, however their dispersion relation is largely altered by the interference of those vertical Bloch modes. HCGs have been reviewed by Chang-Hasnain and Yang.[7] RWGs can have geometries consisting of high contrast dielectric stripes surrounded by lower refractive index geometries, which are similar to HCGs (Figure 1d). Here we define RWGs based on their physical behavior, relying on a leaky guided mode propagating over several grating grooves and ridges, rather than on a particular geometry. This definition of RWG based on their physical behavior is necessary due to the continuity between corrugated waveguide geometries and discrete ribbon geometry as illustrated in Figure 1b,d, and already computed by Knop using rigorous computations in 1981.[8]

The very high bandwidth provided by thin-film dielectric waveguides has been investigated from the 1960s for light transport, especially for on-chip optical interconnects. Dakss et al. have experimentally replaced the conventional prism coupler with a grating coupler for thin dielectric films under laser illumination, using the leaky mode in-coupling of an RWG.[9] A few weeks later, Kogelnik demonstrated a similar light coupling using a gelatin volume hologram.[10] These two early demonstrations gave rise in the 1970s to intense research aiming at fully understanding

G. Quaranta, G. Basset, Dr. B. Gallinet
Centre Suisse D'Electronique et de Microtechnique SA
Muttenz Center
Muttenz 4132, Switzerland
E-mail: bgt@csem.ch
G. Quaranta, Prof. O. J. F. Martin
Ecole Polytechnique Fédérale de Lausanne
Nanophotonics and Metrology Laboratory
Lausanne 1015, Switzerland

The ORCID identification number(s) for the author(s) of this article can be found under https://doi.org/10.1002/lpor.201800017

DOI: 10.1002/lpor.201800017

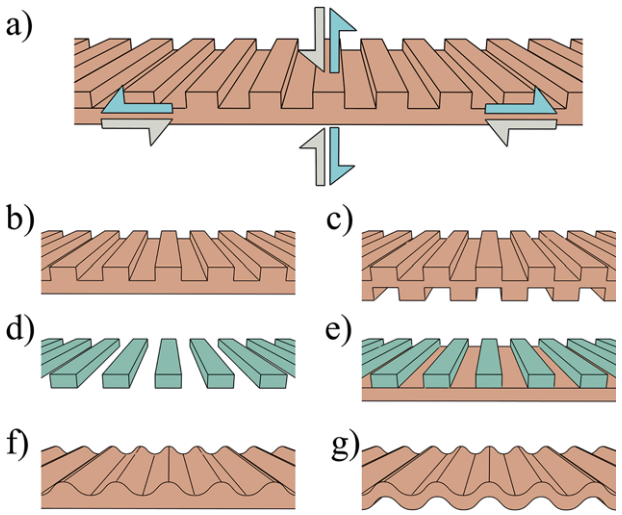

Figure 1. Examples of common geometries of resonant waveguide gratings (RWGs). a) Schematic of the four-port propagation channels, as input (white arrows) or as output (light blue arrows) which are typically used in RWGs. For example, light can be incident from free space, coupled into a waveguide mode, and out-coupled resonantly in specular reflection or transmission. The substrate and superstrate, not represented here, act as a cladding. b) Single-sided rectangular corrugation of a waveguiding layer. c) Double-sided rectangular corrugation with a thin-film waveguide. d) Waveguiding layer corrugated over its full thickness, providing an array of discrete ribbons. e) Array of ribbons on a waveguiding layer. f) Single and g) double-sided sinusoidal corrugation of a waveguiding layer.

the properties of these grating couplers in parallel to the development of distributed feedback mode selectors in laser media.[11,12] Ostrowsky and Jacques measured on a photoresist waveguide–grating coupler the TE/TM wavelength splitting of the resonance for the fundamental waveguide mode.[13] In 1973, Nevière, Petit, and co-workers developed a rigorous model for the resonances of sinusoidal waveguide–grating couplers in photoresist for transverse electric (TE) polarized light,[14] transverse magnetic (TM) polarized light,[15] and the computation of the coupling coefficient for finite beams[16] which were confirmed with a high accuracy with experimental data provided by Jacques and Ostrowsky.[17]

RWGs have also been extensively investigated for their response in the zeroth order of reflection and transmission. Knop provided a first rigorous model for binary structures such a grating lamellas made of high refractive index dielectrics,[8] setting the basis of the rigorous coupled wave analysis (RCWA) modal method; he used this model to compute the zero-order resonances and reflective spectra for a large number of more complex geometries of RWGs.[18] In order to allow affordable and high-throughput manufacturing, he proposed a thin-film coating of a waveguiding layer on a subwavelength-period grating, creating a double-corrugated interface geometry as sketched in Figure 1c,g. Sychugov and Tishchenko demonstrated the TE to TM polarization conversion of light using conical (non-collinear) incidence orientation.[19,20] Gobulenko and Avrutsky observed the same resonances using a thin deposited ZnO-corrugated waveguide,[21,22] achieving much narrower reflection wavelength band in zero-order configuration, thanks to a much lower refractive index contrast of the waveguide. After having studied the first diffracted order resonant anomalies of a multiple dielectric layer coated aluminum diffraction grating, Mashev and Popov demonstrated experimentally similar results with a corrugated waveguide manufactured by ions exchanged from molten $AgNO_3$.[23,24] Avrutsky, Golubenko, and their colleagues computed the zeroth-order reflection and transmission behavior of RWGs and demonstrated their usefulness to stabilize laser emission.[25–27]

Giorgio Quaranta received in 2015 a joint international M.Sc. in micro- and nanotechnologies for ICTs hold in the polytechnics of PoliTo (Torino, Italy), INPG (Grenoble, France), and EPFL (Lausanne, Switzerland). He is currently a Ph.D. student at CSEM S.A. (Muttenz, Switzerland) and a doctoral assistant at the Nanophotonics and Metrology Laboratory in EPFL. His research interests focus on large scale patterning of thin-film metastructures and resonant waveguide gratings oriented toward industrial applications, especially for optical document security, near-eye displays, and spectrometers.

Guillaume Basset is project manager at CSEM Center Muttenz. He is an expert in diffractive and subwavelength optics, resonant waveguide–gratings and micro–nano structuring. He graduated from INP Grenoble, Politecnico di Torino, and EPFL in nanotechnologies for semiconductors. After joining CSEM, he has managed projects on organic semiconductor devices (OLED, OPVs), micro- and nano-optics for various industries such as ultra-short lasers, displays, near-eye-displays, automation, watchmaking, and optical document security. He leads the activities related to resonant waveguide–gratings and optical security at CSEM, continuing more than 30 years of expertise in this field.

Olivier J. F. Martin is professor of nanophotonics and optical signal processing at the Swiss Federal Institute of Technology, Lausanne (EPFL), where he is head of the Nanophotonics and Metrology Laboratory and director of the Microengineering Section. He conducts comprehensive research that combines the development of numerical techniques for the solution of Maxwell's equations with advanced nanofabrication and experiments on plasmonic systems. Applications of his research include metasurfaces, nonlinear optics, biosensing, heterogeneous catalysis, security features, and optical forces at the nanoscale.

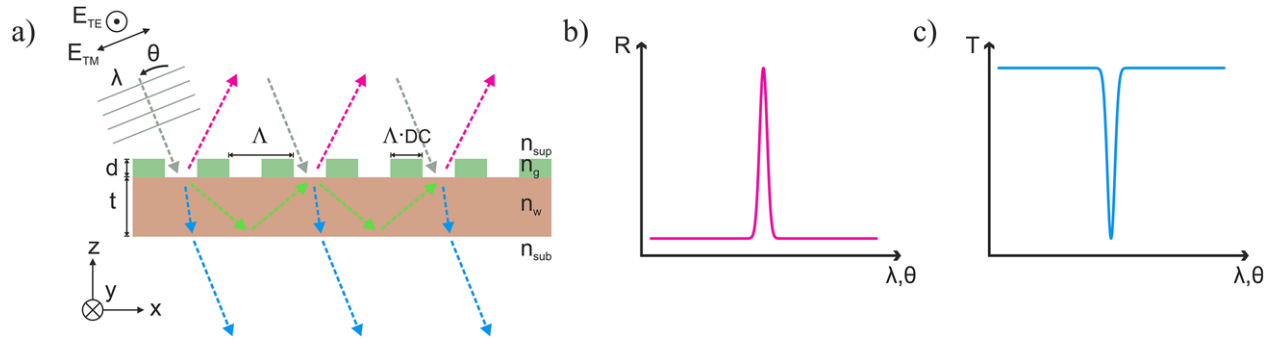

Figure 2. Illustration of a standard RWG. a) Propagation of light rays in the RWG: a complete destructive interference happens in transmission at a specific angle and wavelength of incidence, resulting in a narrowband reflection. An example of b) reflection and c) transmission spectra for polarized light incident at normal at resonance of a monomode RWG.

Overall, RWGs have been investigated by different communities in parallel, leading to a fragmentation of the field since the 1980s and the 1990s after the reviews of the state of the art by Tamir in 1975[28] and by Petit in 1980.[29] In 1997, Rosenblatt et al. reviewed some analytical and numerical models for RWGs that had been developed in the 1980s and 1990s and compared such tools with a series of experimental results.[30] Further conference proceedings were later written by Magnusson et al., presenting properties, applications, and examples of RWGs.[31–35] Several reviews, book chapters, and perspectives specifically focused on the application of RWGs in biosensing have also been written.[36–49] A review of the broader field of subwavelength waveguide structures has been recently published, not including RWGs.[50] Finally, RWGs have been compared with other high contrast metastructures, especially HCGs.[51] Given that context, although a vivid field of research, a comprehensive review of the recent developments and applications of RWGs—from sensing to optical signal processing and optical security—is missing.

1.2. Outline

The aim of this review is to bring together the different communities of fundamental and applied researchers using RWGs and to discuss the latest developments in the field including numerical modeling, manufacturing, underlying physics, and applications of RWGs. Scientists and engineers interested in using RWGs for their applications will also find links to the standard tools and references in modeling, fabrication according to their needs. Section 2 reviews the different numerical modeling methods used to design and optimize gratings, and more particularly RWGs. A few relevant equations and schematics as well as examples are provided to the readers to build their understanding of each approach, its advantages and limitations. The most popular methods specific to the simulation of diffraction in gratings are RCWA and the Chandezon method (C-method). Other popular methods which have been developed for the simulations of photonic structures can be directly applied to the simulation of RWGs: they include volume and surface integral methods, the finite difference in time domain (FDTD), and finite elements (FE) methods. Section 3 provides an overview of the different fabrication methods for RWGs, from the origin with interference lithography, electron beam lithography, or laser ablation to recent manufacturing techniques such as etching, nanoimprint lithography (NIL), and thin-film deposition. In Section 4 specific optical effects which can be obtained using RWGs, including filtering, focusing, field enhancement and nonlinear effects, magneto-optical Kerr effect (MOKE), or electromagnetically induced transparency (EIT) are reviewed. Finally, Section 5 addresses the current applications of RWGs. Thanks to their high degree of tunability in terms of optical properties and the variety of possible fabrication processes and materials, RWGs have been implemented in extremely diverse applications: refractive index and fluorescence biosensors, solar cells and photodetectors, signal processing, polarizers and wave plates, spectrometers, active tunable filters, mirrors for lasers and optical security. Finally, some concluding remarks are given and perspectives for future research and developments around RWGs are discussed in Section 6.

1.3. Fundamentals of RWGs

An RWG can be defined as a thin waveguiding film in optical contact, or merged, with a grating. The waveguiding film operates usually by having a higher refractive index than its surrounding media (the cladding), and because of its thin dimension supports a discrete number of guided modes. The waveguide modes can be limited to the fundamental (zeroth mode) in very thin waveguides or comprise a few modes having different mode indices for TE and TM polarizations. In the latter case, for a given polarization and wavelength, an RWG can support various guided modes having a different mode index and therefore transverse propagation speed and momentum. Light can be coupled into the waveguide modes by different grating diffraction orders, depending on the incidence angle and the wavelength (**Figure 2**a). Some of this guided light is diffracted out of the guide while propagating, coupled back to radiation, and interferes with the non-coupled reflected or transmitted waves, as illustrated with blue and magenta arrows in Figure 2a. Depending on the wavelengths, this leads to a very high reflection or transmission, giving rise to a Fano lineshape profile or Lorentzian like at the zeroth-order reflection (Figure 2b,c). Those efficient resonances can be as narrow as 0.1 nm linewidth[30] and are very sensitive

to angle and wavelength, with a typical angular to spectral linewidth ratio of 0.1° nm^{-1}.[52] Depending on the wavelength and phase delay accumulated during propagation in the waveguide, the destructive interference can occur either in reflection or in transmission.[25,53,54] RWGs are therefore effective filtering structures, especially for collimated light. Further, RWGs can be designed to be extremely efficient diffraction elements of the Littrow configuration as demonstrated experimentally by Destouches et al.[55] Additionally, because the structure consists usually of dielectric materials only, it can be highly transparent and therefore used either in transmission or in reflection. Moreover, RWGs do not suffer from thermal heating such as metallic structures,[56] which enable their use in a variety of high optical power applications such as mirrors and diffractive elements.[57] Each ridge and groove corrugating the waveguiding layer (Figure 1b,c,e–g), or each of the discrete ribbons (Figure 1d) of RWG can be considered a scattering element connected to a thin-film waveguide, making a periodic array of scattering elements in which quasi-guided modes, or leaky modes, can propagate. RWGs can therefore be considered as temporal or spatial optical integrators[58] as well as be used to enhance local electromagnetic field, as examples for sensing[44] and nonlinear optics.[59]

In case of a shallow grating depth d or when the grating is separated from the waveguide by a low-index separation layer, the waveguide mode is weakly perturbed by the grating because of the weak scattering by grating ridges and grooves, and it can be approximated to the one of a pure slab waveguide. Under this assumption, the equation describing modes in a slab waveguide can be coupled with the diffraction grating equation, by setting the propagation wavevector of the mode in the slab waveguide to be equal to the wavevector of the light diffracted by the grating.[60]

$$\begin{cases} \text{For TE modes}: \ \tan(\kappa_i t) = \dfrac{\kappa_i(\gamma_i + \delta_i)}{\kappa_i^2 - \gamma_i\delta_i} \\ \text{For TM modes}: \ \tan(\kappa_i t) = \dfrac{n_w^2\kappa_i\left(n_{sub}^2\gamma_i + n_{sup}^2\delta_i\right)}{n_{sup}^2 n_{sub}^2\kappa_i^2 - n_w^2\gamma_i\delta_i} \end{cases} \quad (1)$$

where

$$\begin{cases} \kappa_i = \sqrt{n_w^2 k^2 - \beta_i^2} \\ \gamma_i = \sqrt{\beta_i^2 - n_{sup}^2 k^2} \\ \delta_i = \sqrt{\beta_i^2 - n_{sub}^2 k^2} \\ \beta_i = k\left(n_{sup}\sin\theta - m\dfrac{\lambda}{\Lambda}\right) \\ k = \dfrac{2\pi}{\lambda} \end{cases} \quad (2)$$

where λ is the wavelength, θ is the polar angle of illumination, Λ is the grating period, m is the grating diffraction order, t is the waveguide thickness, and n_{sup}, n_w, n_{sub} are the refractive index of the superstrate, waveguide, and substrate, respectively. Using this model, it is possible to evaluate a first approximation of the waveguide thickness and of the grating period to obtain a resonance peak for a specific geometrical configuration of the incidence light. An example of a weakly corrugated RWG studied using Equations (1) and (2) is shown in **Figure 3**: the agreement between numerical simulations made with RCWA (described in Section 2.1) in Figure 3a and Equations (1) and (2) in Figure 3b is excellent. Evaluated reflection spectra are shown in Figure 3c at different waveguide thicknesses: when the waveguide is very thin, only the fundamental waveguide mode propagates and gives rise to a single peak in reflection at normal incidence. Conversely, when a thicker waveguide is used, multiple modes can be excited simultaneously at different frequencies. Furthermore, plots of field profiles of the RWGs at different waveguide thicknesses but at the same wavelength and polarizations are shown in Figure 3d–f: their profiles are very similar to the ones of slab waveguides.

A shallower grating depth is used to make higher quality factor Q and narrowband resonances: a deeper grating height causes larger coupling and larger scattering losses leading therefore to a lower quality factor and broader resonances (see Section 4.1). For binary gratings, the duty cycle DC, corresponding to the fill factor of the ridges, is also an important parameter to define the coupling factor, and in turn the bandwidth of the resonance: the case of $DC = 0.5$ allows for maximum coupling and linewidth.[61]

When the grating depth is deeper and has more influence on the profile of the waveguide mode, it is possible to define an equivalent homogeneous layer using the effective-medium theory (EMT)[62–64] to compute the effective refractive index n_{eff} to be used in Equations (1) and (2) in place of the refractive index of the waveguide n_w. The EMT provides a more accurate evaluation of the mode indices for both significantly corrugated waveguides and discrete ribbon geometries, however it is only valid for subwavelength structures.

2. Numerical Modeling

Numerical modeling of RWGs is an important step for the design and can provide quantitative information such as diffraction efficiency and fabrication tolerances, especially for complex or realistic structures where analytical models cannot be directly applied. The optimization of photonic and plasmonic arrays for a specific figure of merit, such as the field enhancement or the diffraction efficiency, can be accelerated using specific optimization algorithms,[65] such as genetic algorithm[66] or particle swarm optimization (PSO).[67] Nevertheless, the fairly large amount of calculations to find an optimal design requires significant computational time and over the last decades, it has been necessary to develop and improve numerical techniques. A variety of methods is available for the numerical simulation of the optical properties of optical micro- and nanostructures, and more specifically RWGs. In this section, the most widely used methods are reviewed. Emphasis is placed on two modal methods, which are specific, highly efficient, and have become the standard methods for the simulation of gratings: the RCWA and C-method. Other popular methods which have been developed for the simulations of photonic structures are highly versatile and can be applied to the simulation of gratings: they include volume and surface integral methods, FDTD, and FE methods. They will be briefly discussed at the end of this section.

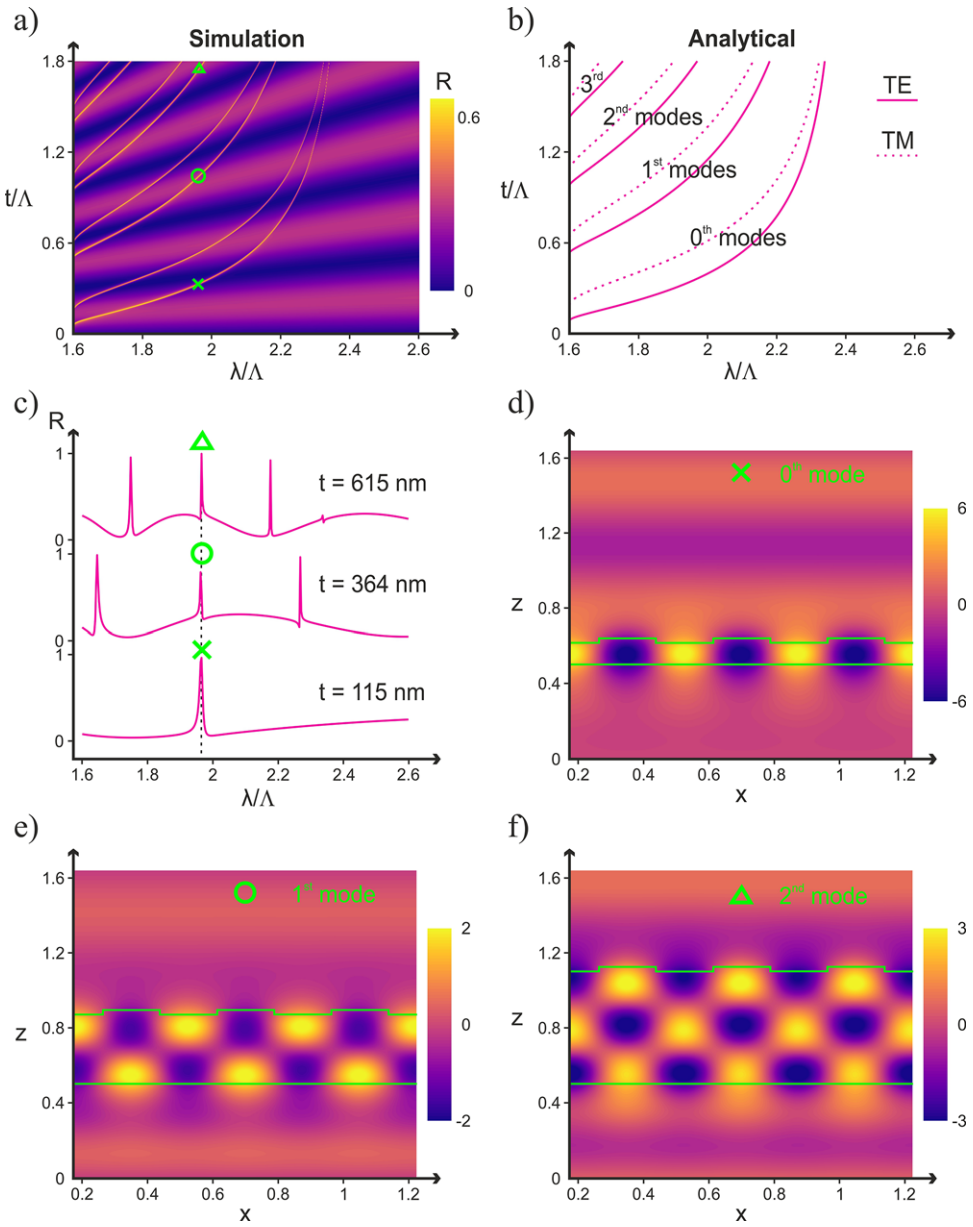

Figure 3. Example of RWG with the following parameters: $\theta = 0^{\circ}$, $\Lambda = 350$ nm, DC = 0.5, $d = 25$ nm, $n_{sub} = 1.6$, $n_w = n_g = 2.4$, $n_{sup} = 1$. a) RCWA simulations of the reflectance at different wavelengths λ and waveguide thicknesses t for both polarizations TE and TM averaged. b) Equations (1) and (2) implemented for this example in reflection for $m = \pm 1$, showing an excellent agreement with the simulations for the prediction of the resonant peaks. c) Reflectance under TE polarized incidence at three different waveguide thicknesses: $t = 115$ nm, $t = 364$ nm, $t = 615$ nm. d–f) Steady-state field profiles $\Re[E_y/E_0]$ under TE polarized incidence at the three waveguide thickness values previously listed at the same resonance wavelength $\lambda = 687$ nm, corresponding to the resonance of the fundamental, first and second excited modes, respectively.

2.1. Rigorous Coupled Wave Analysis

The RCWA, also known as coupled wave method (CWM), modal method with Fourier expansion (MMFE), or Fourier modal method (FMM), is among the most popular numerical methods for the simulation of optical gratings. It mainly consists in expending the dielectric permittivity function of the grating and the electromagnetic fields in the plane of the grating using Fourier harmonics, and enforcing boundary conditions at the different interfaces. A first derivation of this method can be attributed to Knop for a binary transmission phase grating.[8] We would like to provide here a formulation example of the method to give the reader a first view on its advantages, limitations, and challenges. Additional details as well as alternative formulations are provided in the cited references.

A linearly polarized electromagnetic wave is incident at an arbitrary angle of incidence θ and at an azimuthal angle ϕ upon a binary dielectric or lossy grating. The grating period Λ is, in general, composed of several regions with different refractive indices (**Figure 4**a).

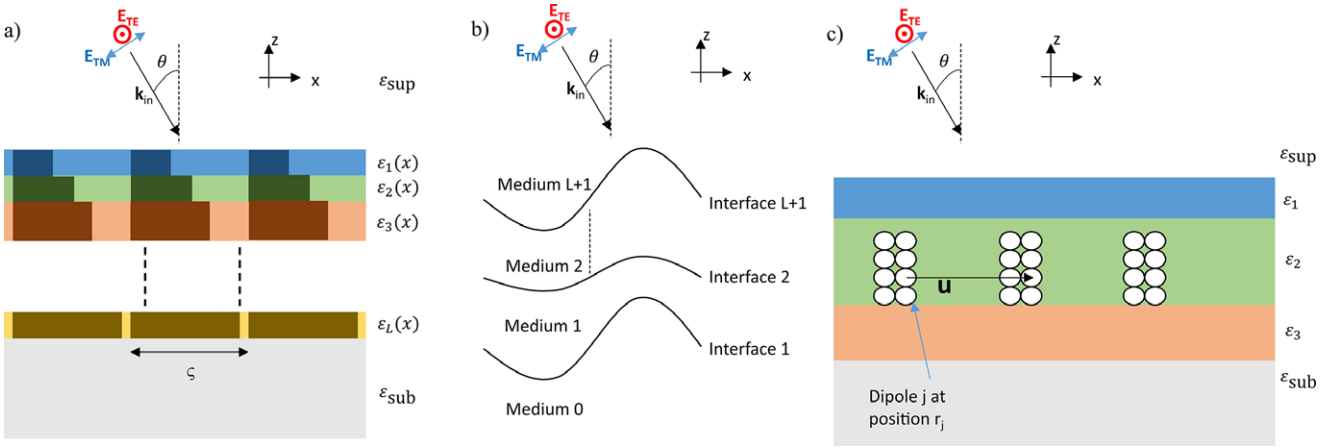

Figure 4. a) Example of approximation of the permittivity function of a blazed grating in an RCWA approach. The grating would be decomposed in different layers, leading to a staircasing effect of the slope. Each layer l of the permittivity function $\varepsilon_l(x)$ is decomposed in Fourier harmonics. b) Definition of interfaces and profiles for the C-method. A change of coordinate is applied to each interface and the problem is solved in the new coordinate system. c) Definition of interfaces and geometry for the periodic form of the discrete dipole approximation (DDA) or volume integral equation. Periodic scatterers are decomposed in discrete dipoles while the response of the background is solved semi-analytically through the computation of Green's function.

The permittivity inside the grating region is expanded into Fourier harmonics in each layer indexed by l.

$$\varepsilon_l(x) = \sum_{n=-N}^{N} \epsilon_{n,l} e^{i\frac{\pi n x}{\Lambda}} \tag{3}$$

where $\varepsilon_{n,l}$ is the nth Fourier harmonics of ε_l. Similarly, the electromagnetic field is expanded in Fourier harmonics in each layer. Applying Maxwell's equations results in a wave equation which can be solved numerically by calculating the eigenvalues and the eigenvectors associated with a $(2N+1)\times(2N+1)$ matrix in each layer, where $2N+1$ is the number of harmonics retained in the field expansions, in general both propagating and evanescent. The space harmonics of the tangential magnetic and electric fields in the lth grating layer are represented in terms of the calculated eigenvalues and eigenvectors. Different matrices with different conditioning are generated with TE or TM polarizations. The reflected and transmitted diffracted amplitudes are obtained by enforcing the boundary conditions at the boundaries between the grating layers. For surface-relief structures divided into L grating layers, this overall results in an additional $2(2N+1)(L+1)$ system of equations to be solved.

During the last decades, extensive work has been conducted in order to improve the convergence of the method and extend its application domains. In 1995, Moharam and co-workers assessed the convergence rate of the RCWA method for single gratings with binary profiles for TE and TM polarizations under collinear and conical incidences.[68] Tests of numerical stability include energy conservation and convergence to the solution (obtained with an infinite number of harmonics) with the increasing number of field harmonics. In the RCWA method, energy conservation is automatically ensured but the number of field harmonics influences its distribution among the different diffraction orders. According to ref. [68], the required number of field harmonics in order to have convergence increases with the grating depth and period; while this number is of the order of a few harmonics when both grating depth and period are comparable to the wavelength (i.e., $\Lambda \cong \lambda$), it can increase to several tens of harmonics for very deep and large gratings (i.e., $\Lambda \gtrsim 10\,\lambda$). Furthermore, a larger amount of orders are required for convergence in TM polarization. In ref. [69], the RCWA is extended to deep multi-level gratings using a transfer matrix approach corrected for numerical instabilities associated with lossy layers or total internal reflections. The RCWA convergence rate has also been drastically improved by several groups in 1996 for the TM polarization using a reformulation of the eigenproblem using a different operator, improving the conditioning of the matrix for TM polarization and thus making the number of diffraction orders required to achieve convergence similar for both TE and TM polarizations.[70–72] Nevertheless, the case of highly conductive gratings with TM polarization still shows some instabilities which have been suppressed by filtering spurious modes,[73] but at the cost of a lower convergence rate. In order to increase the computing resources, RCWA has also been adapted to a cloud computing environment.[74]

More recently, an extensive effort has been undertaken to extend the RCWA method to finite systems, such as grating with a finite number of periods. A relatively straightforward approach is the use of supercells. In this geometry, the cell is composed with all the periods of the scatterer as well as empty space on the cell sides, in order to minimize the effect of the periodicity thanks to the decay of the field in the empty sides. This method it is however not rigorous, in the sense that the radiation condition is imposed indirectly by expanding the computational domain.[75] Guizal et al. have developed a method called aperiodic RCWA (ARCWA), which can be applied to an aperiodic lamellar structure under a finite size beam illumination.[76] The electromagnetic field in the grating and in

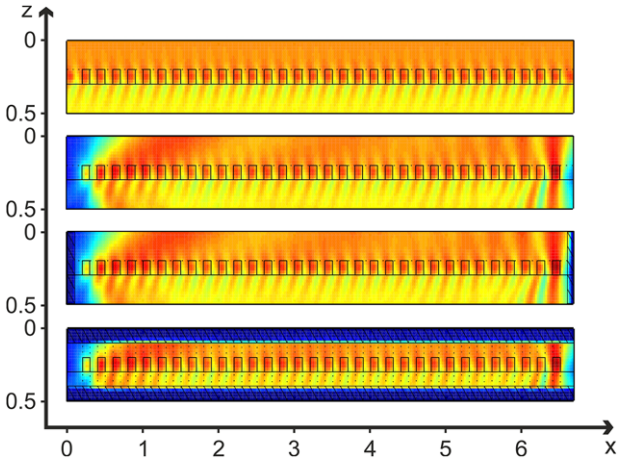

Figure 5. Example of computation of the response $\Re(E_y)$ of a 32 line grating using different methods. From top to bottom: standard RCWA applied to an infinite grating; supercell RCWA; ARCWA with PMLs on the side and layering along *z*-direction; aperiodic RCWA with PMLs on the bottom and top and layering along *x*-direction. Adapted with permission.[75] Copyright 2014, Elsevier Ltd.

the surrounding medium is expressed in terms of Fourier integrals, leading to an integro-differential equation which can be solved numerically using a discretization in Fourier space; note that several hundreds of harmonics are required for convergence of the solution. Lalanne and co-workers have introduced the use of absorbing boundary conditions and perfectly matched layers (PMLs) at the boundaries of the unit cell in order to build and numerically analyze finite structures.[77,78] A review of different approaches for ARCWA is given by Pisarenco and Setija.[75] **Figure 5** shows an example of computation for the fields in a finite grating with 32 lines using different ARCWA approaches and comparing the solution to the standard RCWA. The radiation field in homogeneous space is also calculated using these different approaches (not shown here). The supercell approach requires as expected a large number of Fourier harmonics. The ARCWA approach with PMLs is the closest to the exact solution and does not require a large computational domain. An in-depth complexity analysis is also conducted in this reference.

2.2. Chandezon Method

The coordinate transformation method has been proposed in 1980 by Chandezon and co-workers and is a very well-known method for modeling surface-relief gratings.[79,80] Its main strength resides in its applicability to both TE and TM polarizations with similar convergence rates. The essence of the C-method is to apply a curvilinear coordinate transformation in order to transform a continuous grating profile into a planar surface, therefore facilitating the treatment of boundary conditions. The fields in all media indexed by l are expressed in the following variables (Figure 4b).

$$v = x; u = z - a_l(x); w = y \tag{4}$$

where $a_l(x)$ is related to the profile of the lower interface of layer l. The fields F are expressed as a Fourier expansion in the variable v.

$$F(u, v) = \sum_{n=-N}^{N} F_n(u)\, e^{ik_n v} \tag{5}$$

where

$$k_n = k_x + n\frac{2\pi}{\Lambda} \tag{6}$$

and k_x is the x-component of the incident wavevector and n is the Fourier harmonic. The wave equation for the magnetic or electric field is expressed in terms of the variables u, v, and w and projected onto the Fourier basis. This yields an eigenvalue problem that is similar for both TE and TM polarizations. The method is very efficient if the profiles are identical in each layer (such as conformal films on a surface-relief grating), since the resulting linear system of equations has a number of unknowns scaling with the number of Fourier harmonics only, independently of the number of layers. In its more recent formulation for multilayered systems with arbitrary shapes, a system of equations has to be solved in each layer in a similar way to RCWA, therefore increasing the complexity.[81] The difficult case of sharp edges leading to discontinuities in the structure profile has been treated by replacing them with steep slopes.[82]

Vallius has carried out a comparison between the C-method and the RCWA for the difficult case of TM polarization in conducting multilevel gratings.[83] Although the RCWA is recognized to be more versatile in terms of geometries, polarization, and illumination conditions, it is reported in this reference that the C-method outperforms RCWA in terms of computation time and reliability for these cases because its convergence is by essence similar for TM and TE polarizations.

2.3. Integral Methods

The discrete dipole approximation (DDA), also known as coupled dipole method (CDM) developed by Draine and Flatau considers scattering objects in homogeneous space as a collection of dipoles.[84,85] The method has been later extended to periodic arrays,[86] periodic arrays with a defect,[87] and periodic arrays in multilayered systems.[88] The method has the advantage of rigorously modeling radiative boundary conditions, like modal methods. Compared to grating modal methods, this method can be applied to a very broad range of periodic structures, including inhomogeneous and anisotropic scatterers without increase in complexity. However, the computational effort scales rapidly with the size of the scatterers. Integral methods have been reviewed in more detail for nanophotonics.[89]

We describe below the method formulation for a periodic array of scatterers in a multilayer environment (Figure 4c). Assuming that a single scatterer is composed of M subunits at position $\boldsymbol{r}_i$, the electric field in the unit cell of the periodic structure excited by

an incident electric field E_0 is given by the following expression.

$$E(\boldsymbol{r}_i) = E_0(\boldsymbol{r}_i) + \sum_{j=1}^{M}\left[\sum_{m.n=-\infty}^{+\infty} G(\boldsymbol{r}_i, \boldsymbol{r}_j + m\boldsymbol{u} + n\boldsymbol{v})\, e^{i\boldsymbol{k}_b\cdot(m\boldsymbol{u}+n\boldsymbol{v})}\right] \times \alpha(\boldsymbol{r}_j)\, E(\boldsymbol{r}_j) \quad (7)$$

where $\boldsymbol{k}_b$ is the Floquet–Bloch wavevector associated with periodic boundary conditions, $\boldsymbol{u}$ and $\boldsymbol{v}$ the lattice vectors, α_j is the dynamic polarizability tensor of subunit j, and G is Green's tensor of the multilayered system. Although very versatile, such an integral method has a computational cost since a full system of equations needs to be inverted, which scales rapidly with the size of the scatterers. This approach is also well suited to study finite size gratings in different dimensions.[90–92]

Another family of integral methods uses the method of moments (MoM) to solve integral equations at the boundary surfaces between homogeneous domains. In ref. [93] a MoM is applied to binary gratings embedded in a multilayered medium. Popular in the microwave range,[94,95] the surface integral equation method has been extended to the optical range for the simulation of general 3D photonic and plasmonic crystals.[96] This approach has the advantage of reducing the computational cost as the computation is restricted to surfaces of the scatterers, but is restricted to piece-wise homogeneous scatterers.

For a periodic system, the computation of each matrix element requires an infinite sum, each term involving the computation of Green's tensor. For a homogeneous medium, the Green tensor can be expressed analytically; this is no longer the case in a stratified background, where Green's tensor must be computed numerically—usually in the spectral domain using numerical integration in the complex plane—which has an additional, non-negligible, computational cost.[97] In periodic systems with a homogeneous background, the computation of a periodic Green's function also requires the truncation of an infinite sum of terms, which converges slowly and requires an extensive computational power. Efficient acceleration methods using a Fourier expansion exist, such as Ewald's method.[96]

2.4. Finite Differences in Time Domain

The finite differences in time domain (FDTD) method is one of the most popular methods in photonics because of its ability to handle a large variety of problems,[98] including both periodic and non-periodic structures. In this method, both time and space are discretized, that is, all spatial and temporal derivatives in Maxwell's curl equations are replaced with finite difference quotients. Time domain methods such as FDTD can handle a variety of large systems as they do not require the solution of a linear system of equations, and can be coupled with other equations, such as the equation for the dynamics of population inversion in a laser. However, they also face some challenges, like the implementation of dispersive materials or periodic boundary conditions for broadband sources at non-normal incidence.[99] Furthermore, the calculation of radiative fields is not straightforward compared to, for example, the modal methods previously discussed because FDTD assumes a finite window of computation. In order to simulate open boundary conditions, PMLs are used; they are built from layers of lossy material with a perfectly matched interface that should not reflect a plane wave for any frequency, angle of incidence, and polarization. PMLs can be seen either as coordinate stretching in the frequency domain or as an artificial anisotropic absorbing medium.

2.5. Finite Elements

The finite element (FE) method is another popular differential method in photonics, which allows for accurate computation of the electromagnetic field, originally in the frequency domain.[100] Hybrid and time domain methods based on FEs include the finite elements in time domain method (FETD) and the discontinuous Galerkin time domain method.[101] In contrast to FDTD, the use of basis functions enables the accurate description of the geometry of micro- and nanostructures, which can be crucial when studying the influence of nanoscale variations of shapes on the electromagnetic response.[89,100] The modes as well as their resonance frequencies, losses, and spatial extension can be directly calculated. The high accuracy of the computed electromagnetic field allows studying the electromagnetic confinement in nanostructures and in particular the influence of geometrical parameters on the near-field distribution.[102]

3. Fabrication Techniques, Implementations, and Materials

Advances of RWGs have not only been boosted by increases in computational power and improved modeling algorithms as outlined in Section 2, but also thanks to the developments of several microfabrication and nanofabrication techniques. In particular, new mastering techniques have provided microstructures and nanostructures of higher quality and with increased reproducibility and homogeneity, while replication and fabrication techniques have allowed higher throughput, lower costs, and better accuracy from research and development to industrial production.[103,104] In parallel, various characterizations, metrology and quality control techniques have also been developed.[105,106] Section 3.1 presents different origination techniques of gratings: laser interference lithography is a standard process in case of periodic and uniform large areas (Section 3.1.1), while electron-beam lithography is more suitable when the pattern is not uniform or homogeneous (Section 3.1.2). Other mastering techniques are employed for specific requirements, that is, laser ablation (Section 3.1.3). The mastering of the grating usually includes the etching process to transfer the pattern of the photoresist into the substrate (Section 3.1.4). The thin-film deposition techniques are discussed in Section 3.2. For high-throughput or cost-efficient requirements, the master grating is replicated by NIL (Section 3.3).

3.1. Grating Mastering and Low-Throughput Fabrication Techniques

3.1.1. Laser Interference Lithography

A very common technique for the manufacturing of periodic and large scale gratings is holographic lithography, or laser

interference lithography.[107] It is a technique based on recording the standing wave of an interference pattern between two or more coherent laser beams with a photosensitive material such as a photoresist. The holographic exposure of such a thin-film photoresist layer allows the manufacturing of various grating structures, usually periodic and with sinusoidal or quasi-sinusoidal topographies. Note however that this approach is highly insensitive to misalignments and the development of the photosensitive material development critical to achieve the desired grating profile and depth. Yet, this approach can be pushed to the extreme and it is possible to create sub-50 nm period patterns by using extreme ultraviolet holographic lithography at synchrotron radiation facilities.[108]

3.1.2. Electron Beam Lithography

When non-periodic patterns or smaller patterns are required, the electron beam lithography is also a standard origination technique, typically affordable for samples up to a few square centimeters.[109] It is the preferred technique when the RWG pattern is not uniform or homogeneous.[110] Electron beam lithography allows to precisely control the duty cycle DC[111] and to achieve sub-10 nm grating lines.[112,113] However, since large patterns require the stitching of multiple deflections field of an electron beam, stitching errors can create irregularities in the pattern for sample dimensions in the hundred micron to millimeter scales.[114] Recent developments for large-area electron beam exposure have reached exposure speeds of 1 min mm^{-2} for non-tilted gratings with a 560 nm period,[115] and 3 min mm^{-2} for tilted gratings with a 200–500 nm period.[116]

3.1.3. Laser Ablation

Laser ablation is a versatile fabrication technique to generate surface-relief gratings directly on many materials—including high damage threshold materials—without any need for further etching. Direct laser writing allows a sequential patterning while the exposition of excimer lasers or ultra-fast lasers through a photomask allows parallel processing. Laser ablation may however suffer from the accumulation of redeposited debris particles around the ablation site.[117] Using F_2 laser at 157 nm, submicrometer RWGs were realized with a grating depth in the 5–50 nm range.[118] A grating–interferometer setup can further improve the quality of gratings made via laser ablation.[119]

3.1.4. Anisotropic Etching

Anisotropic etching is performed to remove a residual photoresist layer, to deepen or modify the grating profile—for example, reaching steep profiles such as binary gratings—or to transfer the grating into the underlying material—for example, the waveguiding layer. It is realized by various ion beam etching (IBE) processes relying on material sputtering and using chemical reactivity to increase the material selectivity and etching speed as in reactive ion etching (RIE) or using an accelerated ionized beam as in reactive IBE (RIBE)—also called ion beam milling. Such processes are carried out in vacuum chambers in which a plasma is created using a single gas or multiple gases. The throughput is relatively low and anisotropic etching is generally used for microstructure mastering and the fabrication of high added-value devices. As illustrated in **Figure 6**, specific algorithms based on the string method have been developed to simulate the structural deformation of the grating profile during the etching process and to more accurately predict the fabricated optical behavior.[120] The presence of unetched residual layers between the gratings and the waveguide can lead to a shift of the resonance wavelength[121] due to change of guided mode effective index as for a mismatch in the waveguiding layer thickness or refractive index, and conversely, in the case of over-etching, a shift of the resonant peak is also expected.[122,123]

3.2. Deposition Techniques

Deposition techniques such as chemical vapor deposition (CVD), physical vapor deposition (PVD), plasma deposition,[124] atomic layer deposition (ALD),[125] or RF sputtering allow the creation of waveguiding layers with high uniformity and accuracy, as well as multilayer stacks. The waveguiding layer(s) define primarily the guided mode effective index, and therefore the resonance frequency; accurately controlling the deposition is critical in many applications. Such techniques can be used both at wafer level and in high-throughput coating techniques such as roll-to-roll PVD, following roll-to-roll grating replication using NIL. It is possible to fabricate a position variable RWG filter by sputtering a graded thickness waveguide.[126] An oblique angle layer deposition is suggested to improve the sensitivity of RWG sensors.[127] The deposition rate is also uneven and highly sensitive to experimental conditions (Figure 6).[120]

3.3. Nanoimprint Lithography

High-resolution (sub-10 nm) NIL has been used for more than 20 years[128,129] as a low-cost technique compatible with high-throughput manufacturing to replicate nanostructures.[130] Many different process flows and replication techniques are gathered under the name NIL. An example is the casting or coating of a sol–gel material on a PDMS soft replica to replicate the structure on glass or thin-film polymer[131] after UV or thermal curing and annealing.[132,133] Another widely used implementation is hot-embossing based on a negative replication stamp made of nickel and various additives. For high-throughput replication of grating patterns, sheet to sheet and preferably roll-to-roll NIL or injection molding[134] techniques have been industrially applied,[130,135] especially for biosensing,[136] optical security,[137] and solar cell applications.[138] In order to improve the replication fidelity and to broaden the range of geometries and aspect ratios that can be replicated, UV reticulation of liquid, gel, or soft materials (UV-NIL) is preferred to hot-embossing techniques and

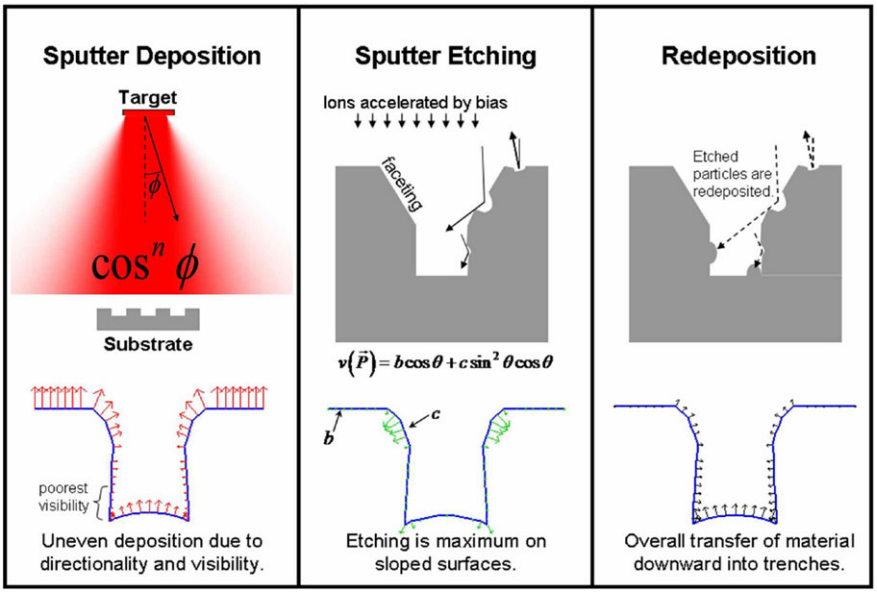

Figure 6. Three main sources of errors in sputter deposition and etching processes and their modeling: deposition (left panel), etching (middle panel), redeposition (right panel). During sputter deposition, most of the neutral particles are deposited to the substrate with vertical diffusion, however a small amount diffuses at oblique angle, causing deposition on the sidewalls. During the etching process, materials are removed with an angular selectivity, thus the sloped surfaces have higher etch rates. Part of the material removed during etching can be redeposited back onto the surface. Reproduced with permission.[120] Copyright 2007, Optical Society of America.

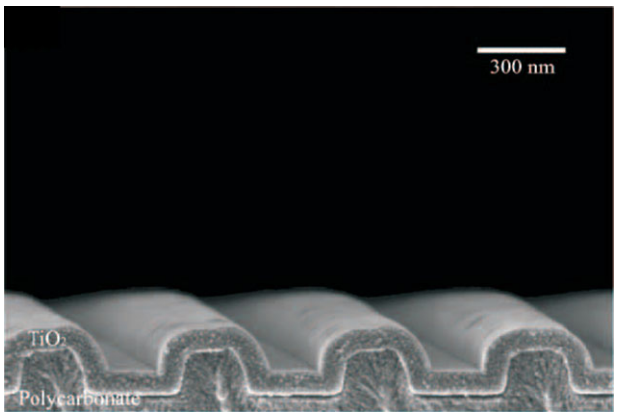

Figure 7. Example of a replicated grating on polycarbonate, coated with TiO_2. Reproduced with permission.[143] Copyright 2012, Optical Society of America.

gradually replacing them in many industries. Recent variations on NIL include stretchable molds to replicate the grating with the desired period,[139,140] multiple-mold replica NIL to reduce the grating depth,[141] or doped NIL to fabricate RWG in one step without the need for any further deposition.[142] An example of a replicated grating on polycarbonate by hot-embossing followed by deposition of TiO_2 is shown in **Figure 7**.

4. Effects Associated with RWGs

RWGs make use of a grating to couple light in and out of a thin waveguide. As already briefly outlined in the introduction, RWGs have been designed in a variety of operational modes beyond the functionality of a mere grating coupler. This section reviews the main effects which have been obtained using RWGs: they include narrowband or broadband filtering in the zeroth order of transmission and reflection, combination with surface plasmon resonances (SPRs), focusing, field enhancement, and nonlinear effects as well as other effects such as MOKE or EIT. As will be seen in this section, the design rules for RWGs, materials, and the parameter range generally depend on the targeted optical effect and the fabrication constraints. Guidelines specifically addressed for the design of narrowband filters are proposed by Nieder et al.[144]

4.1. Narrowband and Broadband Filters

The bandwidth of the filtered spectrum can be made particularly narrow using a weak in-coupling and out-coupling efficiency with, for example, shallow gratings (**Figure 8**a).[30] When used as narrow bandpass spectral filters in either transmission or reflection, RWGs are characterized by a spectral response which can be identified to a Fano lineshape.[54,147–149] RWGs can theoretically reach 100% of reflection efficiency when their profile is vertically or horizontally symmetric[150] or when integrated with quarter-wave Bragg stacks.[54] Recently, a high efficient narrowband transmission filter has been demonstrated with two crossed and strongly modulated RWGs[151] and at normal incidence with partially etched single-layer RWG.[152,153] RWGs can also be utilized to make efficient wideband reflectors using a periodic array of high-index scatterers on a low index layer (Figure 8b,c).[145,146] The bandwidth and the efficiency of the broadband reflectors with partially etched RWGs can be tuned with the grating depth, fill factor, the thickness of the homogeneous layer, and with

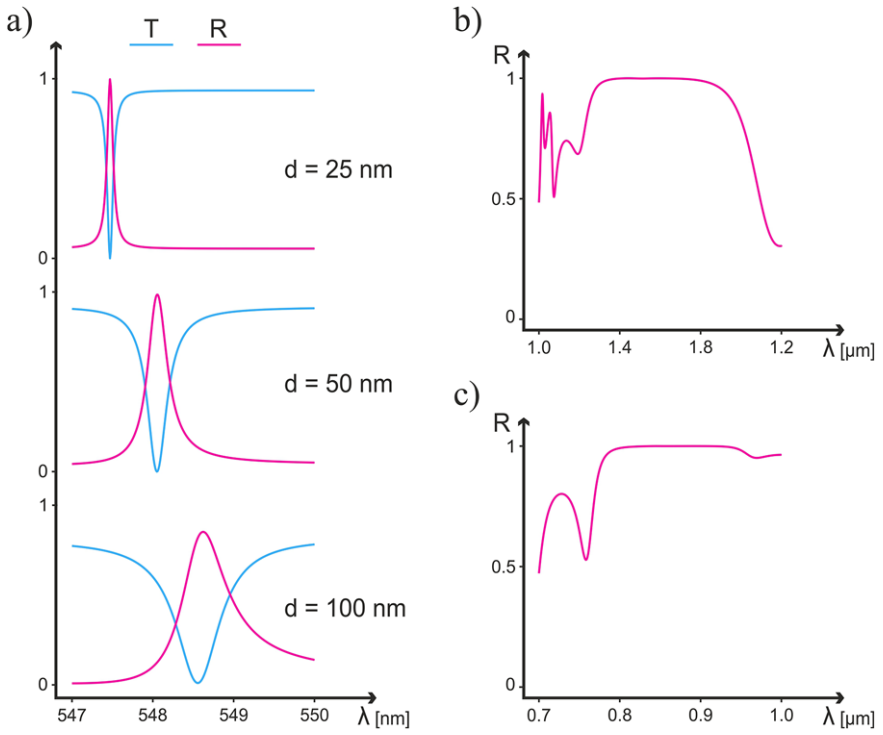

Figure 8. a) RCWA simulations of the grating depth (d) variation to tune the reflection/transmission bandwidth in TM polarization. Parameters: $\theta = 15^{\circ}$, $\Lambda = 400$ nm, $DC = 0.5$, $t = 300$ nm, $n_{sub} = 1.6$, $n_w = n_g = 1.7$, $n_{sup} = 1$. b,c) RCWA simulations of TM polarized broadband RWG reflectors in different IR wavelength ranges. b) Parameters: $\theta = 0^{\circ}$, $\Lambda = 700$ nm, DC = 0.75, $d = 460$ nm, $t = 840$ nm, $n_{sub} = 3.48$, $n_w = 1.47$, $n_g = 3.48$, $n_{sup} = 1$.[145] c) Parameters: $\theta = 0^{\circ}$, $\Lambda = 340$ nm, $DC = 0.68$, $d = 220$ nm, $t = 2\ \mu$m, $n_{sub} = 3.72$, $n_w = 1.454$, $n_g = 3.72$, $n_{sup} = 1$.[146]

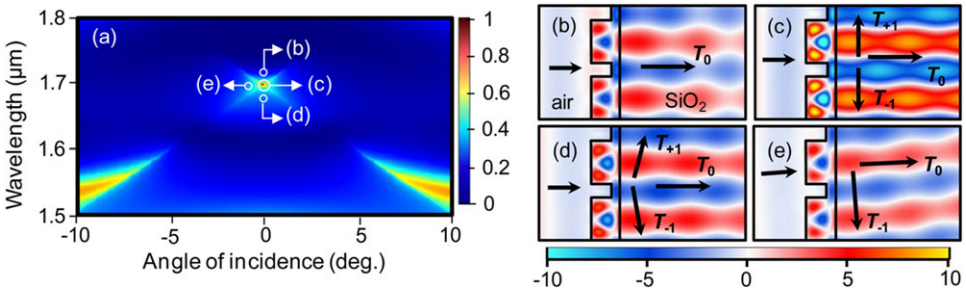

Figure 9. a) Simulated transmittance of an RWG optical filter coupled with Rayleigh anomaly in TM polarization. Parameters: $\Lambda = 1130$ nm, $DC = 0.723$, $d = 405$ nm, $t = 160$ nm, $n_{sub} = 1.5$, $n_w = n_g = 3.48$, $n_{sup} = 1$. b–e) Field distributions for several cases of angle and wavelength as indicated in (a). The case (c) is at the exact resonance condition, and in the case (e) there is a strong transmitted first order that causes a decrease of the zeroth-order transmission. Reproduced with permission.[158] Copyright 2013, AIP Publishing.

tapered sidewalls.[154–156] Efficient wideband reflectors with steep sidewalls can be obtained by operating RWGs at the proximity of the Rayleigh angle.[157] When an RWG resonates at an angle corresponding to the Rayleigh anomaly, the zeroth-order reflection energy is almost completely transferred into a first-order transmitted mode with a sharp transition, as shown in **Figure 9**.[158] The Rayleigh anomaly is related to the rapid efficiency variations of diffraction orders by a variation of the wavelength or the incident angle.[2,159] It occurs for a specific value of angle (θ) and wavelength (λ): $n_{sup} \sin\theta = \pm n_{sub,sup} - m\lambda/\Lambda$, where Λ is the grating period and m is the diffraction order ($m = \pm 1, \pm 2, \ldots$) for reflection and transmission, respectively. This interaction is helpful for designing transmission filters with sharp peaks.[158]

Rahman et al. demonstrated a system of metallic–dielectric grating structures that significantly improves the transmission efficiency by tuning the waveguide thickness to satisfy both the guided mode and the Fabry–Perot resonances at the same wavelength.[160]

We would also like to report the fabrication of wedged RWG used as tunable filers, whose resonance spans over 40 nm in the visible range in the case of 50 nm increment of the waveguide thickness.[161] Other implementations include the patterning of RWG on suspended membranes for improved quality factor and flattened sidebands,[162–164] that is, for laser cavities,[165] and RWGs on concave lenses to increase the resonance wavelength and decrease the linewidth.[166]

Finally, RWGs made with antireflective coating have been studied.[167,168]

4.2. Combination of Guided Mode and Surface Plasmon Resonances in Metallic Dielectric RWGs

Plasmon materials are metals with a very high electron mobility, in excess of 10^{22} cm^{-3}, such that when light impinges on a nanostructure made from such a material it excites a collective oscillation of the free electrons in the metal, called a plasmon resonance.[169] Consequently, the interaction of light with plasmonic nanostructure is extremely strong, leading to very large scattering cross-sections in the far-field and enhancement of the near-field intensity by several orders of magnitudes. Combining plasmonic nanostructures with RWGs has been proposed as early as the 1990s by Parriaux and Voirin, to combine low-loss propagation and high near-field enhancement for sensing applications.[170] Over the last decade, progress in nanotechnology has enabled the seamless integration of plasmonic metals with RWG to take advantage of these features.[171]

Metallic RWGs can combine coupled-mode resonances and plasmonic resonances near the Rayleigh anomaly,[172] thus exhibiting extremely narrow spectral features with a high efficiency.[173] This approach can be used to produce an extremely broad range of colors.[174] It is worth mentioning that these two examples rely on aluminum as plasmonic material less common than gold, which is usually the material of choice for plasmonics, since it is easy for nanofabrication. Nguyen-Huu et al. have used silver to produce broadband and high transmission efficiency color filters;[175] interestingly, these authors also consider an additional dielectric layer on top of the RWG structure, which appears to improve the overall performances. Other authors have taken a different approach and fabricated a device with similar performances using an aluminum grating on an ultra-thin 100 nm silicon nitride membrane.[176] Recently, metasurfaces—optical surfaces that exhibit useful and often uncommon functionalities—have emerged as a strong field of research,[177] which has prompted revisiting many classical photonics devices. RWGs also follow that trend and interesting reports have been published on the combination of gradient metasurfaces with a waveguiding layer.[178] Whilst a conventional grating provides a constant phase gradient to the incoming light, a metasurface has the potential to engineer the phase in a more versatile manner. This phase can also be engineered in two dimensions, contrary to a conventional grating, which is intrinsically 1D. 2D plasmonic RWG devices can exhibit, for example, a useful polarization-sensitive behavior that produces a dichroic response and can be used to engineer electrically tunable filters.[179]

Traditionally, plasmonic nanostructures have been successfully used for sensing.[180] Magnusson and colleagues have reviewed how such nanostructures can be combined with RWG to produce even more efficient and versatile sensors.[181] For example, Chien et al. have shown how coupled waveguide–surface plasmon resonance biosensor can be useful to overcome the limitations associated with Kretschmann attenuated total reflection used on conventional biosensors;[182] as a matter of fact, RWGs maintain their performances, even under normal illumination.

The strong near-field produced by a plasmonic nanostructure can induce interesting optical effects that go beyond light scattering. This has been used by Zeng et al. in an RWG device to boost the photoinduced charge-transfer rate of hot electrons into a semiconductor material.[183]

So far, we have presented some examples of RWGs that incorporate plasmonic elements and rely on the optical resonances that are localized on them (so-called localized plasmon resonances). There exists another family of plasmonic effects, so-called propagating plasmon resonances, that are associated with extended surfaces.[184] Many experiments on propagating plasmon resonances use a grating to excite this optical mode that then propagates on a thin metal film.[185] Sometimes, the mode is out-coupled using a second grating,[186] thus representing a device very similar to an RWG, albeit with an extremely thin metal waveguiding layer.

4.3. RWGs as Focusing Elements

Advanced patterning enables creating beam shaping devices with more freedom in the manipulation of the wavefront, such as for beam steering or focusing. Concentric circular focusing grating couplers have been known since a long time[187–189] and they have been implemented as optical routing, for example, for wavelength division multiplexing (as illustrated in Figure 14g),[190,191] for cavity resonators,[192,193] or for quantum information processing.[194,195] Recent optimizations include circular RWGs on a membrane,[196] apodized focusing grating couplers (sketched in **Figure 10**a),[197] and long working distance gratings.[198] A focusing spatial bandpass transmission filter based on a periodic RWG was also reported with a multilayer geometry allowing broadband reflection sidebands.[153] Instead of curving the grating lines on flat substrates, GMRs can also be created on curved surfaces, such as on parabolic reflectors to create wideband focusing devices (see Figure 10b)[199] or on cylindrical surfaces (see Figure 10c,d)[200] to enhance the quality factor of the related cylindrical cavities[201] by hybrid resonant modes coupled to whispering gallery modes.[202] Fattal et al. demonstrated the possibility of using linear with varying duty cycle or varying period 1D SWG to achieve local control over the phase of the reflected beam, realizing very long focal/small angle beam redirection reflective lenses.[203,204] Given the distributed nature of the resonance in waveguide–gratings, achieving large phase shift at a very small scale, enabling large angle redirection, appears intrinsically difficult with such approaches. More localized resonances such as vertical GMRs present in HCGs and some dielectric metasurfaces appear better adapted. Such an approach was demonstrated with 2D non-periodic SWGs, while additional optical functionalities can be obtained by combining finite size SWGs with different dimensions.[205] Subwavelength structures are able to support to some extent both localized and non-localized quasi-guided resonances, we review here only the latter. A focusing device has recently been demonstrated for operation with low-coherence sources such as white LEDs, by patterning two impedance-matched RWGs (Figure 10e–h).[116,206] In that geometry, both gratings share a thin high refractive index waveguide and are therefore impedance matched. The direction

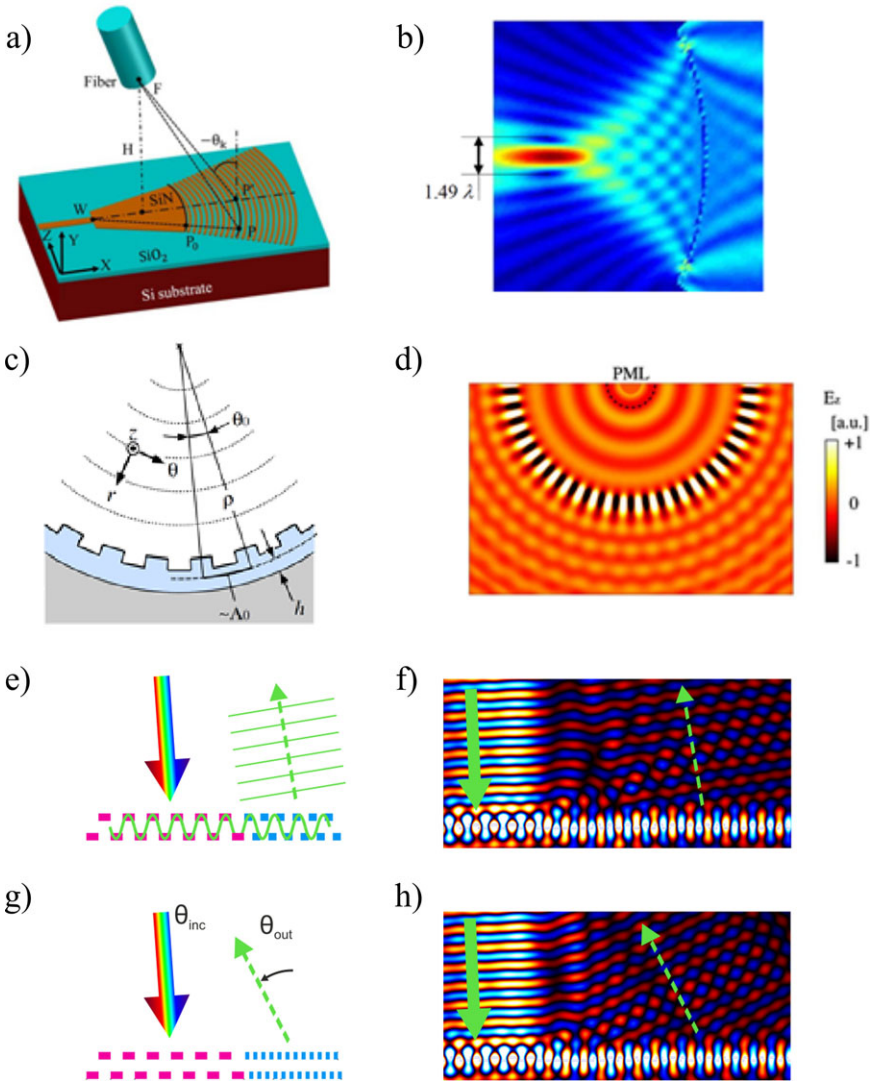

Figure 10. a) Schematics of a self-imaging chip–fiber grating coupler. Reproduced with permission.[197] Copyright 2012, Optical Society of America. b) Electric field around an RWG used as focusing reflector. Reproduced under the terms of the CC-BY 3.0 license (https://creativecommons.org/licenses/by/3.0/).[199] Copyright 2011, the Authors, Published by MDPI. c) Schematic of a curved RWG and d) the electric field at resonance wavelength. Reproduced with permission.[200] Copyright 2011, Optical Society of America. e) Pairs of impedance-matched RWGs for color-selective light redirection. A corrugated ultra-thin waveguide coats a first and a second adjacent grating, schematized, respectively, in pink and blue. A specific wavelength range is in-coupled inside the waveguide by the first grating from a white incident light beam, and out-coupled from the second grating. f) By changing the period of the second grating, it is possible to out-couple the light at a different in-plane angle. g,h) Corresponding amplitude of the transversal near-field obtained with FDTD simulations. Adapted with permission.[116] Copyright 2017, American Chemical Society.

of the out-coupled modes differs from the direction of the incoming light by tuning the period of the second RWG. Since only a single waveguide mode can be excited at a specific wavelength and angle, the device acts as a color-selective redirection element.

4.4. Field Enhancement and Nonlinear Effects

The electromagnetic field confinement in an RWG can be intensified by resonance effects[207] or reduced in the case of strongly modulated waveguides.[208] Bezus et al. have extended the use of the generated evanescent field enhancement (factor of 30) at the resonance condition to obtain high quality interference patterns.[209] This work, targeting contact photolithography to generate small periodic structures, demonstrated numerically field intensity with periods six times smaller than that of the RWG used, much smaller than can be generated with simple periodic structures and Talbot effect.

Nonlinear responses can arise using RWGs thanks to the strong local enhancement of the electromagnetic field in the guided modes.[59] In fact, the periodic corrugation of a waveguide was found to be an efficient method for phase matching nonlinear optical interactions, especially when the period is of the order of one coherence length.[210–213] Applications of nonlinear effects

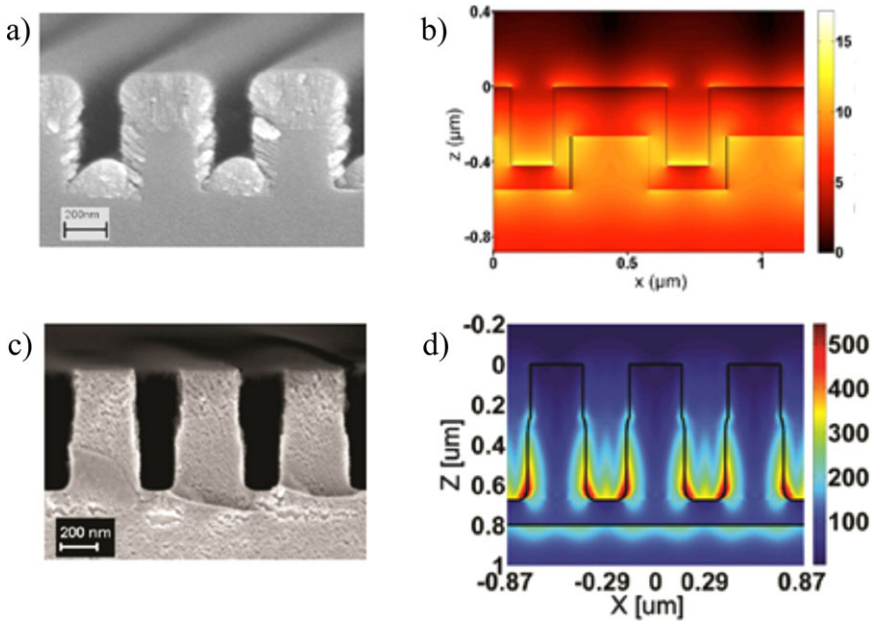

Figure 11. Scanning electron microscope images of a) the TiO_2 grating used for SHG and of c) the SiN grating used for UV THG. b,d) Square of the amplitude of the electric field normalized to the incident field in the vicinity of the RWG structure at resonance. Reproduced with permission.[218,221] Copyright 2007 and 2013, AIP Publishing and Optical Society of America.

enhanced by RWGs in signal processing include switching, computing, and telecommunications.[214] In order to increase the field localization effects and to have phase matching at the same time, the RWG is designed to have its fundamental resonance at the photonic band edge, at which it is optically pumped, and to have a quasi-phase-matched nonlinear substrate.[215,216] The far-field diffraction patterns of the linear (i.e., the fundamental frequency) and the nonlinear (i.e., the second harmonic frequency) beams have been shown to have a clear angular separation because of the diffraction at different angles.[217] The second harmonic generation (SHG) was enhanced by a factor of 550 (**Figure 11**a,b),[218] 1000,[219] and 5500[220] compared to a flat waveguide using only dielectric RWGs and using fabrication methods compatible with CMOS technology.[219] This enhancement is larger than typically observed in metallic nanostructures with plasmonic resonances. Strong UV third harmonic generation (THG) was also enhanced by a factor of 2000 with CMOS-compatible RWGs (see Figure 11c,d).[221] Further studies regarding the influence of the relative orientation of the pump light polarization, grating bars, and crystal axes were recently reported.[222] The generation of SHG and THG with RWGs made with azopolymer as coating material[223] or as waveguiding material in an all-polymer-based RWG[224] were also investigated and further improvements are expected.

4.5. Other Effects

4.5.1. Magneto-Optical Kerr Effect

The MOKE is a weak phenomenon describing the changes of p-polarized light reflected from a magnetized surface.[225] There are three different configurations for MOKE experiments, depending on the direction of the magnetic field with respect to the plane of incidence and the sample surface: polar MOKE, longitudinal MOKE, and transverse MOKE. RWGs are especially used to enhance the transverse MOKE. For the transverse MOKE geometry, the magnetic field is normal to the plane of incidence and only the p-polarization is affected. A small Kerr wavevector is generated parallel to the reflected polarization, which can either increase or decrease the polarization amplitude depending on the direction of the magnetic field. The enhancement of this effect has always been very challenging. Vincent et al. demonstrated the use of RWGs on a nonlinear Kerr media to achieve effective optical bistability and hysteresis phenomena, because RWGs increase the local field and thus the nonlinearities.[212] Recently, an RWG made from alternating magneto-insulating and nonmagnetic dielectric nanostripes achieved a large magneto-optical Kerr response that can improve high-definition imaging, magneto-optical data storage, and magnonics.[226]

4.5.2. Equivalent of Electromagnetic Induced Transparency

EIT is an important phenomenon associated with the formation of a narrow transparency window in the spectral region of a broad absorption band, which causes a remarkable reduction of the light group velocity; it is caused by quantum destructive interference between different excitation pathways in multi-level atomic systems.[227] An equivalent of the EIT spectral response can be realized by combining an RWG and a slab waveguide (**Figure 12**a). The incident light is efficiently coupled in the RWG. The light guided in the RWG is weakly coupled to the slab waveguide through its evanescent field. An interference between light which has been indirectly coupled in and out from the slab waveguide through the RWG with the light which has been only in and out

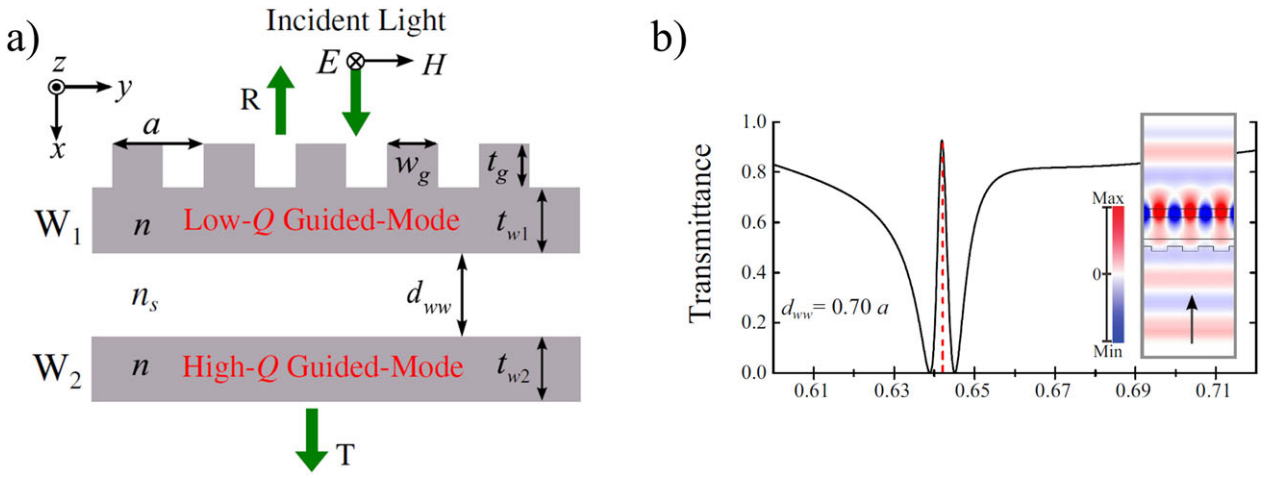

Figure 12. a) Schematic of an RWG configuration used to achieve the equivalent of EIT spectral response. b) Simulated transmission spectra of the proposed configuration: a narrow transparency window is present. The inset shows the electric field distribution. Reproduced with permission.[230] Copyright 2015, Optical Society of America.

coupled in the RWG occurs, resulting in a narrow transmission window[228–230] (Figure 12b). A 2D RWG can be used to generalize this effect to a polarization-independent equivalent of EIT.[231]

5. Applications

As discussed previously, RWGs can be used as coupling and waveguiding elements, near-field enhancers, zeroth- or higher-order diffraction elements, and filters with a tailored control of the intensity and phase of the diffracted optical fields. Thanks to their high degree of tunability in terms of optical properties and the diversity of fabrication processes and materials involved, RWGs have been implemented in many different applications. In Section 5.1, their use in refractive index and fluorescence biosensors is reviewed. RWGs to enhance the light absorption of thin-film solar cells and photodetectors are presented in Section 5.2. Their implementation in signal processing for photonic integrated circuits and optical communication is discussed in Section 5.3. Polarizers and wave plates designed with RWGs are outlined in Section 5.4. Passive RWG filters can be implemented for spectroscopic applications (Section 5.5), and active RWG filters as electro-optic or thermo-optic tunable filters (Section 5.6). Their use as narrowband reflectors has also enabled the design of efficient mirrors for laser cavities (Section 5.7). Finally, their use in optical security devices, which represent an established and widespread industrial application, is reviewed in Section 5.8.

5.1. Sensors

In 1983, Lukosz and Tiefenthaler discovered that a thin (i.e., 120 nm) monomode SiO_2-TiO_2 RWG was sensitive to changes of relative humidity in air.[232,233] In this experiment, the grating had a finite size and was used as waveguide coupler. The variation of the effective refractive index of the guided modes was related to the adsorption of the gas molecules on the waveguide surface and the consequent variation of the refractive index of the cladding material. In 1992, the first implementation of a full RWG (i.e., where the grating is not only used as in-coupler but also as leaky out-coupler) in sensing was proposed by Magnusson and Wang.[234] The basic RWG filter was shown to exhibit sensitive shift in wavelength on a change of refractive index and the results as RWG sensor were later published by Wawro et al.[235] This concept has been further developed and applied to produce compact and inexpensive commercial sensors.[236–238] The utilization of RWGs as refractive index biosensors is discussed in (Section 5.1.1) and that of fluorescent RWG sensors in Section 5.1.2. Some possible configurations are sketched in **Figure 13**.

5.1.1. Refractive Index Biosensors

As a result of the binding of molecules on an RWG surface, the effective refractive index (n_{eff}) of the guided mode of an RWG varies, producing a shift in the resonance wavelength.[44]

$$n_{\text{sup}} \sin\theta = m\frac{\lambda_0}{\Lambda} - n_{\text{eff}} \tag{8}$$

where n_{sup} is the refractive index of the superstrate, θ is the waveguide coupling angle (i.e., in-coupling or out-coupling depending on the configuration), m is the diffraction order, λ_0 is the wavelength in vacuum at which the maximum coupling and resonance occurs, and Λ is the grating period. An analytical model based on a slab waveguide, where the propagation constant has additional constraints, can be used to predict, with an accuracy of 0.45 nm across the visible spectrum, the resonance shift caused by the refractive index changes that is valid even for deep grating modulation.[240] Furthermore, the phase of the out-coupled pattern is also a useful source of information: Mach–Zehnder interferometers based on RWGs have been designed[241] and Sahoo et al. have recently proposed an analytical model to evaluate the phase and shown its importance in refractive index sensing.[242] Many different implementations of RWG have been suggested to create portable and label-free biosensors; they

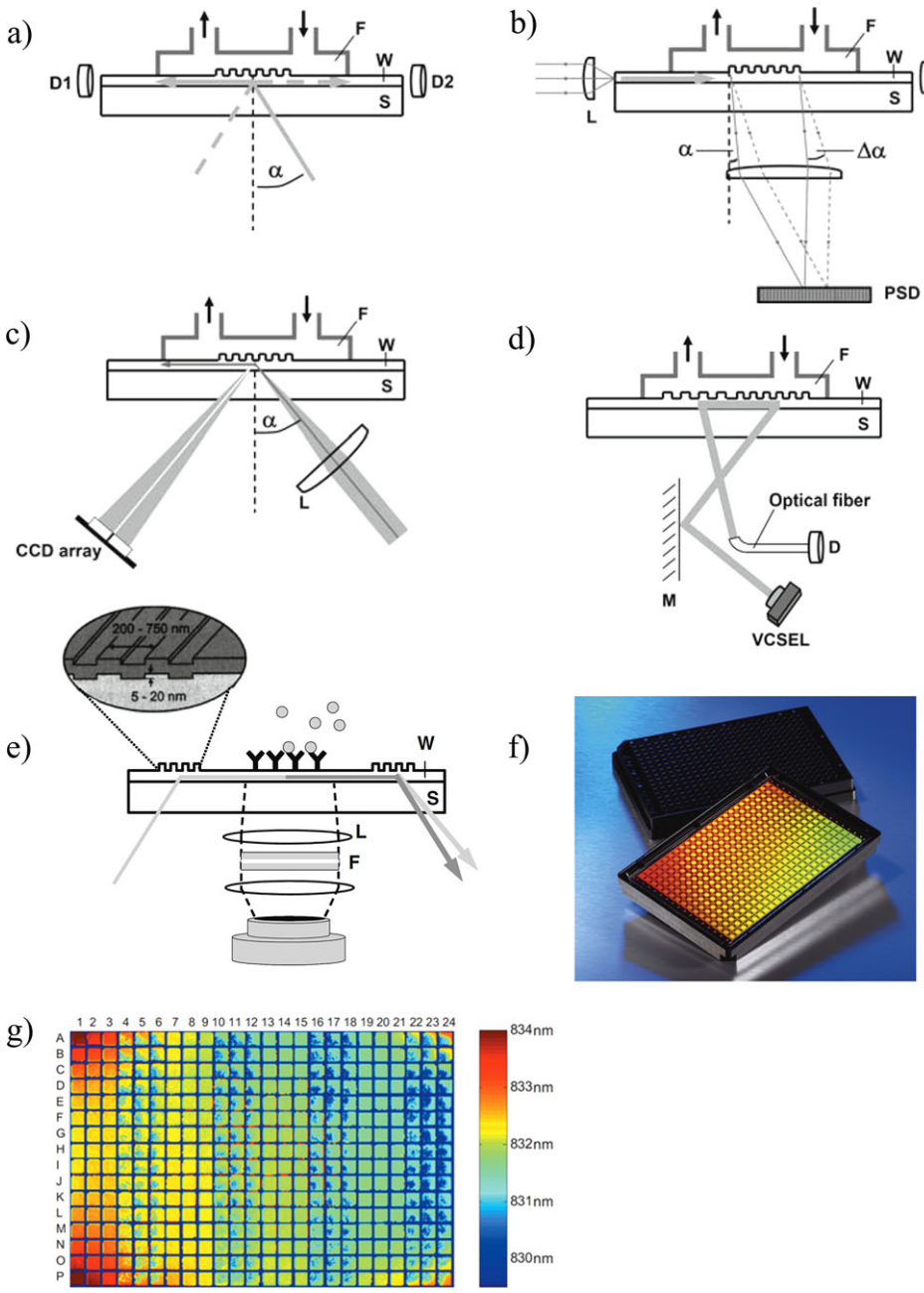

Figure 13. Schematic drawings of some different RWG configurations for sensing: a) an input grating coupler, in which an RWG grating is used to couple light in the waveguide, which is then sensed, and, conversely, b) an output grating coupler. c) A reflected-mode grating coupler similar to (a) but sensing the reflection spectra. d) A wavelength interrogated optical sensor (WIOS), made by two different RWGs to sense the back-scattered light at a different angle and e) an evanescent-field fluorescence, made with two RWGs separated by an intermediate flat waveguide. Reproduced with permission.[44] Copyright 2010, Springer-Verlag. f) A Corning Epic 384-well RWG biosensor plate, each containing an independent RWG biosensor allowing high-throughput screening of intractable targets. Reproduced with permission.[36] Copyright 2006, Elsevier Ltd. g) A false-colored image of the resonance wavelengths of that plate after overnight culturing of human epidermal carcinoma cells planted in different conditions. Reproduced with permission.[239] Copyright 2010, AIP Publishing.

all rely on a strong spatial overlap between the RWG evanescent wave and the analyte. Compared to other methods for detecting the refractive index change (e.g., interferometric systems), RWGs are usually less sensitive because of the shorter interaction length. On the other hand, they support a higher-throughput detection system and they can be implemented in practical and less expensive sensing applications, since they are less sensitive to ambient or sample temperature fluctuations.[44]

Let us mention for the interested reader the several specialized reviews on RWG biosensors. Cooper reviewed optical biosensors made with different technologies (plasmon resonance, waveguides, and resonant mirrors)[243] and compared advantages and

drawbacks of labeled assays and label-free assays[36] including RWG biosensors and a list of manufacturers. An example of application of a commercial RWG biosensor for live cell sensing is illustrated in Figure 13f,g,[239] where different colors show different resonance wavelengths depending on the different culturing conditions of the cells. Fang et al. reviewed optical biosensors for cell sensing and their potential implications in drug discovery, for which RWGs biosensors are presented as being the most popular ones, together with SPR biosensors.[37,41] Fang et al. also authored two book chapters reviewing RWG biosensors for whole-cell assays for drug discovery[42] and RWG biosensors with high-throughput analysis.[244] More details on modeling and mechanisms for RWG biosensors are described in refs. [38,39,44], while different practical implementations are reviewed in refs. [40,44, 45]. RWGs have been used in fragmented-based drugs screening in both academic and industrial projects.[43] Geschwindner et al. have written a focus on small-molecule screening with RWGs biosensors; they emphasize the specific advantages of the inhibition in solution assay, in contrast to traditional direct binding assay.[46] Recent label-free silicon-based optical biosensors, including RWG-based biosensors, and their implementation into lab-on-a-chip platforms have been reported by Gavela et al.[48] Finally, a recent review from Paulsen et al. about RWG biosensors is focused on compact readout systems for point-of-care applications and the implementation of multiperiodic and deterministic aperiodic RWGs in order to design specific resonances.[49]

5.1.2. Fluorescence Enhancement

RWGs have been known to confine and enhance the electromagnetic field at resonance, which makes them interesting for fluorescence enhancement. Fluorescence is widely used in the field of optical biosensing, mainly thanks to its exceptional sensitivity.[249] Particularly effective is the two-photon fluorescence (TPF) spectroscopy, where two photons of half the energy are used to excite the fluorophore that emits a fluorescent photon with higher energy, thus providing low background noise and excitation wavelength in the near-IR. It is possible to use RWGs to enhance TPF without the need for highly focused laser excitation light, with an enhancement in excess of two orders of magnitude compared to the case of a flat waveguide.[250–252] RWGs are also a powerful tool for the detection of extremely small TPF signals generated by picosecond laser pulses.[253] The near-field nature of the fluorescent enhancement by an RWG was experimentally verified by measuring the enhancement factor as a function of the distance and comparing the results to numerical calculations,[254] showing that the exponential decay length is mainly controlled by the resonance wavelength of the RWG. Applications of this fluorescent enhancement are foreseen in biosciences and medicine,[255] for example, to detect androgenic anabolic steroids used illegally as growth promoters.[256,257] Further improvements of RWG-enhanced fluorescence include the implementation of a quartz substrate to improve the detection sensitivity and signal-to-noise ratio[258] and the growing of a highly porous waveguiding layer to increase the surface area and to allow fluorophores to penetrate into the most sensitive region of the RWGs.[259]

5.1.3. Absorption Sensors

Visual chemical sensors based on resonant absorption conditions of RWGs have been developed to create low-cost gas and fully passive detectors with significantly improved color change compared to thin dye-containing films. They can be used to monitor gas contamination in public places in case of terrorist attack, gas leakages in possible explosive environments, air pollution as well as the vibrational absorption of molecules.[136,260]

5.2. Absorbers, Solar Cells, and Photodetectors

Efficient thin-film solar cells are designed by enhancing the light optical absorption in order to achieve efficient photon-to-electron conversion using approaches based on slow light. Although the slow-light effect is intrinsically bandwidth limited, it has been demonstrated that RWGs can be effectively used as slow-light propagators that elongate the optical path length and enhance light trapping in solar cells in the near-IR[261] or visible band[262] and decrease light reflection. In particular, the GMR is used to reduce the penetration of the field in the substrate by forcing the diffraction of the field to propagate laterally in the RWG layer and thus increasing the optical path inside the absorbing layer. Lee et al. proposed an RWG with two filling factors to improve the angular acceptance and thus the light trapping in solar cells, as asymmetric RWGs are more angular tolerant.[261] Moreover, the functional principles of RWGs as absorbing media can be extended to two dimensions for both TE and TM polarizations without substantial changes.[263–266] Further improvements of such an RWG absorber include the optimization through a genetic algorithm[267] or by implementing a two-step design approach using two different numerical modeling, that is, with an iterative Fourier transform algorithm (IFTA) to optimize the transmission function followed by RCWA optimizations to improve the absorption,[263] or by using first RCWA to design the RWG and later an FDTD analysis to evaluate the absorption.[268] The implementation of a backside metal reflector has been shown to further raise the absorbance.[102,267] Finally, the experimental observation of a single waveguide mode enhancing the light-trapping effect through a 2D RWG was recently carried out with a scanning near-field optical microscopy (SNOM).[269]

Another implementation is related to coherent perfect absorbers (**Figure 14**a–c), which are lossy structures that allow a complete absorption of coherent illumination, as the time reversal of a laser having the opposite (positive) imaginary part of the refractive index of its gain medium.[270] A coherent perfect absorber based on a thin-film a-Si RWG using two TM polarized beams has been developed.[245,271] Since coherent absorbers do not require nonlinear effects to actively modulate light intensity, they can be used as low power active devices such as optical switches, modulators, light–electricity transducers, and coherence filters for IR detectors.[245]

High speed optical photodetectors are highly valued components for optical data communication. It is possible to increase the bandwidth efficiency of very compact photodetectors compatible with standard CMOS processes with a germanium-on-insulator 2D RWG, in which the field decays after only a few

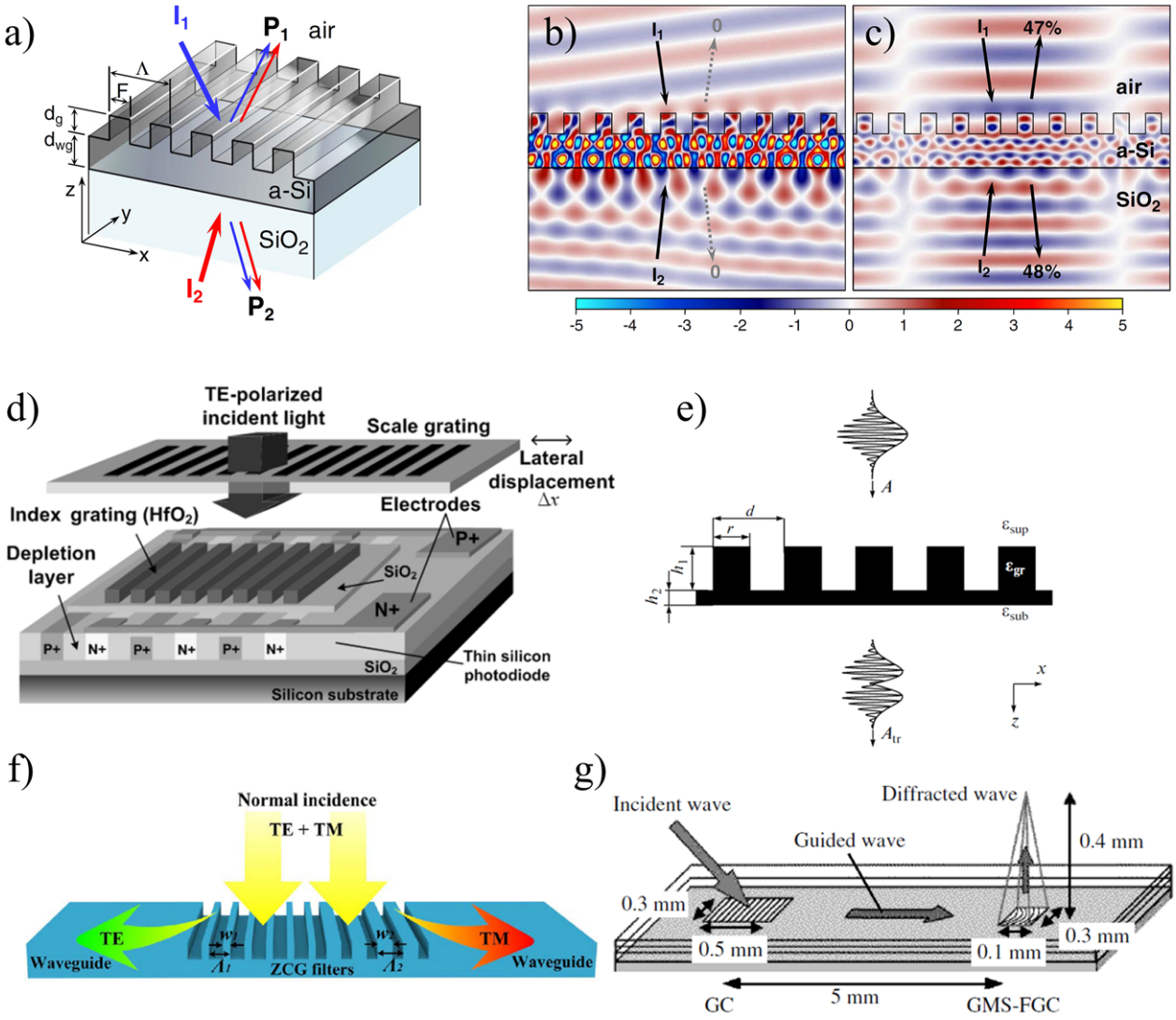

Figure 14. a) Illustration of a coherent perfect absorber. b) Magnetic field pattern when the two TM beams are in in-phase incidence and c) when they are out-of-phase incidence. Reproduced with permission.[245] Copyright 2014, Optical Society of America. d) Illustration of a micro-displacement encoder using an RWG photodetector. Reproduced with permission.[246] Copyright 2007, IOP Publishing Ltd. e) Schematic of an RWG used for differentiating an incident pulse. Reproduced with permission.[247] Copyright 2012, Pleiades Publishing, Inc. f) Schematic of a polarization beam splitter. Reproduced with permission.[248] Copyright 2016, Elsevier Ltd. g) Schematic of a focusing grating coupler. Reproduced with permission.[190] Copyright 2004, IEEE.

grating periods enabling high external quantum efficiencies.[272] A more rectangular spectral response can be obtained by cascading double or triple RWGs.[273] A photodetector in the mid-IR region can also be realized with a germanium grating on a CaF_2 waveguide to narrow the photoresponse spectral range enabling mid-IR sensing applications.[274] An optical displacement encoder aimed at converting mechanical displacements into electrical signals has been designed with an RWG photodetector based on a Moiré configuration with two superimposed gratings, consisting of an RWG to detect only the ± 1st-order beams diffracted from a scale grating movable with two piezo actuators, as illustrated in Figure 14d.[246] Finally, a photodiode for ambient-temperature detection has been realized with an InGaAs detector integrated with a dielectric RWG to enhance the absorption at the backside.[275]

5.3. Optical Communication and Signal Processing

Photonic integrated circuits or integrated optical circuits are devices which integrate two or more photonic functions in a similar way to integrated electronic circuits, but using photons rather than electrons. Relaxed latency, wide bandwidth, and high resistance to electromagnetic interferences are some of the promising driving forces behind the development of such platforms.[276] As discussed earlier, RWG were initially developed as thin-waveguide couplers in the 1970s following the work of Dakss et al.[9] and the state of the art was reviewed by Tamir in 1975[28] and by Petit in 1980.[29] Optical interconnects with higher efficiency and lower coupling losses than using micro-mirrors have been measured.[277] Recent RWG developments have focused on signal processing for photonic

integrated circuits and optical communication, especially with emphasis on compatibility with CMOS technology. The following implementations are described here: differentiators and integrators (Section 5.3.1), wavelength-division (de)multiplexers (Section 5.3.2) and polarization beam splitters (Section 5.3.3).

5.3.1. Differentiators and Integrators

The differentiation of optical signals is of great interest for ultra-fast all-optical information processing, analog–optical computing, optical recognition and coding, and temporal pulse shaping.[58,278] RWGs are particularly attractive for these optical operations because the Fano profile describing the reflection or the transmission coefficient of the structure near the resonance can approximate the transfer function of a differentiating filter.[279,280] The differentiation of an optical signal can be performed as temporal or spatial differentiation. The temporal differentiation consists in the differentiation of the pulse envelope, while the spatial differentiation consists in the differentiation of the spatial profile.[58] The first theoretical demonstration of temporal differentiation of optical signals using an RWG was carried out by Bykov et al. (Figure 14e).[247,278,281] They demonstrated that an RWG operating in transmission allows the calculation of the first-order derivative and integral of an optical signal envelope around the Wood anomaly and the fractional derivation and integration of order 1/2 around the Rayleigh frequency. They further explained a method to design stacked RWGs with k resonances to compute the kth-order derivative.[282] The spatial differentiation of optical beams have been studied by Golovastikov et al. by converting a 2D Gaussian beam into a 2D Hermite–Gaussian beam with an RWG in transmission geometry.[58] They also presented a planar differentiator with a two-groove RWG operating in reflection to be used as a resonant integrated spectral filter for optical pulses and beams propagating in the waveguide.[279] New devices for optical pulse transformation, in optical information processing problems, and analog optical computations, are also foreseen.[283]

5.3.2. Wavelength Division (de) Multiplexers

The design of integrated devices having ultra-broadband bandwidth usually requires high wiring density and increased data rates, which cause the pin-bottleneck problem. Optical interconnection offers promising solutions for the signal transmission.[284] Among different implementations, RWGs are an effective way to make such kind of devices with reasonable width and sideband levels for the multiple channels: this need was one of the major driving forces behind the initial research on RWGs in the 1970s.[28] Moreover, RWGs provide thermal stability, robustness, and ease of fabrication, since the performance of a single RWG corresponds to tens of traditional thin-film layers.[285] A possible way to create a wavelength division (de)multiplexer is to use different gratings to in-couple, out-couple, and focus multiple wavelengths at different locations (see Figure 14f);[190,191,286–288] a small aperture compatible with the beam size of a single mode vertical cavity surface emitting laser can be necessary.[289] Another possibility is to use very thick waveguides in order to benefit from multiple diffraction orders and GMRs.[290,291] Wavelength division (de)multiplexers can be fabricated on silicon wafers and operate with visible light by suspending the structure[248] .

5.3.3. Polarization Beam Splitters

RWGs can efficiently be used as polarizers and, therefore, they can also be implemented to create functional polarization beam splitters for optical interconnects. The first experimental demonstration of a bi-wavelength polarization splitter with RWGs on a silicon on insulator platform was achieved by Streshinsky et al.[292] Silicon-based RWG can also be used to perform simultaneous focusing and polarizing beam splitting of an unpolarized Gaussian beam. RWGs with multiple periods, as shown in Figure 14f, have been recently developed as wavelength division demultiplexers and polarization beam splitters.[248] By properly tuning the thickness of the waveguide and the grating depth, a three-port beam splitter with equal efficiencies in the zeroth transmitted, first, and minus first guided orders can be created with a monolithic, encapsulated, single-period grating.[293] The optical functions of mode conversion, polarization rotation, and asymmetric optical power transmission demonstrated on 2D waveguides with phase-gradient metasurfaces[178] could be envisioned as well with dedicated metasurfaces using 1D confined resonant waveguides.

5.4. Polarizers, Depolarizers, and Wave Plates

RWGs are intrinsically angular and polarization-sensitive devices, and therefore suitable to make polarizers, depolarizers, and wave plates. Among the many types of polarizers, wire-grid polarizers are known to work for a relatively broad bandwidth.[294,295] Wire-grid polarizers made with metallic materials have higher losses compared to polarizers made with low-loss semiconductors or dielectrics.[294] Lee et al. have shown that a single RWG layer made with amorphous silicon can provide high transmittance over 100 nm of wavelength range in TE polarization and low transmittance over 40 nm of wavelength range in TM polarization in the telecommunication wavelength range.[296] This range was then extended to 200 nm bandwidth thanks to PSO[297] and with an inverse polarization design.[298] These authors investigated as well the performances of RWG polarizers made with different low-losses materials, such as silicon, silicon nitride, and titanium dioxide.[299] If the RWG is built from a very high-index bimodal waveguide having a deep double-sided corrugation, a coalescence of the reflection peaks of TE0 and TE1 modes suppresses the dip between them, leading to a wideband and wide angular polarizer that works with low temporal and spatial coherence light sources such as LEDs.[300] Ultra-sparse RWGs (illustrated in **Figure 15**a,b) made with a very low duty cycle (10%) can be used as well as effective wideband polarizers and be designed for different spectral domains.[301]

Fully deterministic depolarizers can also be implemented using thin RWGs for quasi-monochromatic light, by

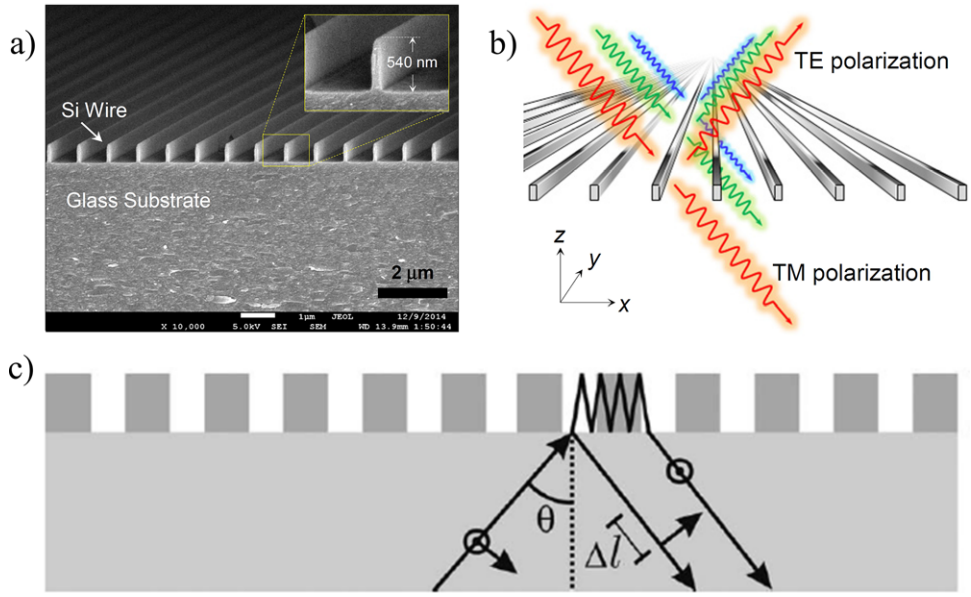

Figure 15. a) The scanning electron microscope image of an ultra-sparse TE reflector and b) its illustration. Reproduced with permission.[301] Copyright 2015, Optical Society of America. c) Schematic of the operation of a pseudodepolarizer. Reproduced with permission.[302] Copyright 2009, Optical Society of America.

implementing a total reflection configuration that lets the guided mode travel longer than the coherence length, as illustrated in Figure 15c.[302] A similar principle can also be used to transfer spatial correlation to partial polarization, enabling a drop in the degree of polarization for the reflected beam.[303] TM to TE polarization rotation could be achieved using conical incidence on an RWG.[19,304] Half-wave and quarter-wave retarders made with RWGS have also been demonstrated.[305]

5.5. Spectrometers

Spectroscopy with RWGs is an application that has been recently emerging, triggered by the need for compact devices which can be satisfied thanks to the use of waveguiding. Several implementations have been proposed using RWGs as waveguide couplers or zero-order filters. A concept of RWG out-couplers to angularly separate the different wavelengths coupled in a waveguide in combination with a plano-convex lens to focus them on a photodetector array has been proposed.[306] Furthermore, the RWGs can be curved in order to directly achieve the focus.[307] Another demonstration of compact a device has been made by printing a customized organic photodetector array on the out-coupling RWG.[308,309] Using RWGs in the zeroth order of diffraction, a possible technique to spatially separate resonance wavelengths uses a gradient in the thickness of the waveguide, reaching a resolution as small as 0.011 nm for the wavelength range between 800 and 900 nm,[310] or alternatively with a gradient in the grating period (**Figure 16**a).[311,312] Mid-IR spectrometers based on RWGs were also reported for infrared spectroscopic imaging using, for example, a filter wheel to sweep for the different bands.[313] Other applications include the measurement of vibrational modes of molecules,[314] while discrete-frequency IR spectroscopy[315] has been used for measurements of tissues and polymer samples and for implementing coherent absorbers.[271] Spectrometers based on RWGs also apply to biosensing with incoherent light and, as an example, they can be implemented with broadband light from external sources (such as LED or incandescent lamps) and the camera of a smartphone, as illustrated in Figure 16b.[316] A recent development of filters realized with RWGs include a stack of two RWGs with a Fabry–Perot resonator to generate a transmission peak[317]: the grating duty cycle and period are controlled to obtain a set of narrowband filters with different central wavelengths.

5.6. Active Tunable Filters

The optical properties or RWGs can be dynamically tuned by implementing active electro-optic or thermo-optic tunable filters. Micro-optical-electro-mechanical systems (MOEMS) and nano-optical-electro-mechanical systems (NOEMS) tunable RWG filters are briefly reviewed in Section 5.6.1, electro-optic and liquid-crystal RWG filters are discussed in Section 5.6.2 and thermo-optic RWG filters are described in Section 5.6.3.

5.6.1. MOEMS and NOEMS Tunable RWG Filters

MOEMS and NOEMS technologies enable the miniaturization and integration of optical systems for a broad variety of applications, including displays, wavelength division (de)multiplexers, optical synthesizers, and optical sensors.[318] The general approach is to take advantage of a dynamic mechanical variation of the grating parameters, for example, the period, to tune a given optical property, for example, the reflection band. An MOEMS structure can be constructed with two silicon-on-insulator

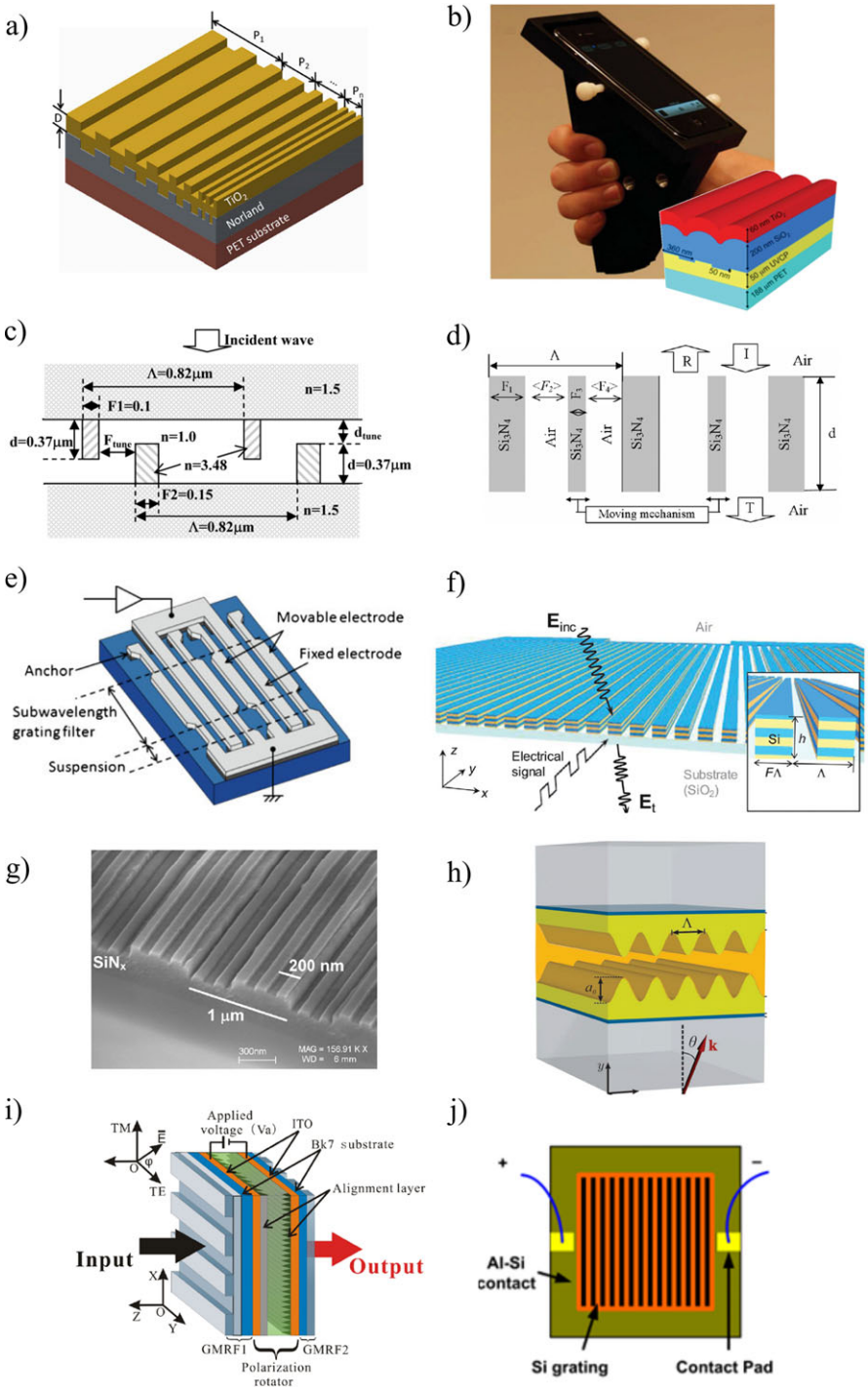

Figure 16. a) Schematic of an RWG with gradient grating period. Reproduced with permission.[311] Copyright 2016, IEEE. b) Spectroscopic biosensor for smartphone application based on RWGs, as illustrated in the inset. Reproduced with permission.[316] Copyright 2013, The Royal Society of Chemistry. Schematic of MEMS tunable RWGs, where the tunable parameter is c) the vertical distance between the two grating layers (Reproduced with permission.[319] Copyright 2006, IEEE) and d) the horizontal distance (Reproduced with permission.[321] Copyright 2007, Optical Society of America). e) Schematic of a NEMS RWG tunable color filter. Reproduced with permission.[324] Copyright 2012, The Japan Society of Applied Physics. f) Schematic of a silicon p–n junction embedded in a subwavelength-grating intensity modulator. Reproduced under the terms of the CC-BY 4.0 license (https://creativecommons.org/licenses/by/4.0/).[328] Copyright 2017, the Authors, Published by Macmillan Publishers Limited. g) Scanning electron microscope image of a superimposed grating made by a double NIL process, where a shallower grating is superimposed onto a deeper grating. Reproduced with permission.[331] Copyright 2007, IEEE. h) Schematic of a zenithal bistable RWG. Reproduced with permission.[335] Copyright 2017, IEEE. i) Configuration of a bandwidth tunable RWG filter. Reproduced with permission.[333] Copyright 2015, Optical Society of America. j) Top-view schematic of a thermo-optic tunable filter in a Joule heating arrangement. Reproduced with permission.[337] Copyright 2013, IEEE.

(SOI) single-layer RWGs, where the relative position between the two layers can be mechanically adjusted, as illustrated in Figure 16c.[319,320] By tuning the horizontal movement, the resonance wavelength can shift across 300 nm in the near-IR range and the reflection efficiency can be optimized by tuning the vertical movement. By implementing an asymmetric RWG having two different dielectric domains per period and by displacing laterally one compared to the other, a tunable MOEMS/NOEMS device has been studied numerically using RCWA (Figure 16d)[321] and is suggested as a tunable pixel for display systems with an angular acceptance tolerance of ±4° or for multispectral imaging applications.[322] In other NOEMS implementations, the displacement between the different RWG lines have been realized with parallel-plate actuators in the infrared to control the reflection band[323,324] or in the visible range to generate a tunable color filter (Figure 16e).[324]

5.6.2. Electro-Optic and Liquid Crystal Tunable Filters

Electro-optic filters use an external electric field to induce a change in the refractive index of semiconductors, which can be used for dynamic modulation of the reflectance, in particular tuning of the resonance wavelength[325–327] (Figure 16f).[328]

Another implementation of electrically driven tunable filters is to integrate liquid crystals in direct proximity to RWGs to modify the waveguide modes indices, since liquid crystals have one of the largest known electro-optic coefficients, or using liquid crystals to control the polarization of light interacting with the RWG. Applying a voltage on twisted nematic liquid crystal molecules placed as a cladding of an RWG allows to tune the resonance wavelength and reflectance[329,330] A short-period grating can be superimposed on a larger-period grating (Figure 16g), in order to increase the strength of the anchoring of the liquid crystal molecules.[331] Liquid crystals have been also used as polarization controllers combined with, for example, a dichroic resonator made of a waveguide and anisotropic nanostructures, in order to generate a tunable and polarization dependent transmission filter.[179] Alternatively, they have been applied to create bandwidth tunable filters by fine tuning the grating parameters to place TE and TM guided modes with different bandwidths at the same spectral position[332] (Figure 16i).[333] The stacking of three different devices allows creating a full-color RGB reflector especially promising in energy-saving display systems.[334] Further research on optimal LC materials are expected in the future. Recently, an improvement on the switching time has been proposed using liquid crystal zenithal bistable, as sketched in Figure 16h.[335]

5.6.3. Thermo-Optic RWG Filters

Thermo-optic RWG filters have a resonance condition that depends on the temperature. A possible implementation is to use the thermo-optic index modulation of a graded-index soda-lime RWG, in order to realize a wavelength shift of 13 pm K^{-1}.[336] It is possible to increase the resonance shift to 0.12 nm K^{-1} with a-Si RWGs and by exploiting the electrical Joule heating, as illustrated in Figure 16j.[337] By using polymer-based RWGs on glass substrates, the thermal sensitivity can be more than doubled, reaching 0.268 nm K^{-1}.[338]

5.7. Mirrors for Lasers

Cavity resonator grating filters made with RWGs offer generally more advantages in terms of fabrication and upscalability compared to conventional multilayer dielectric mirrors, such as distributed Bragg reflectors (DBRs), since they require less deposition layers to reach the same quality factor. HCGs have been reviewed by Chang-Hasnain and Yang especially for their use as mirrors.[7] Application of RWGs as intra-cavity mirrors (Section 5.7.1) are outlined here, as well as their specific implementation as cavity-resonator-integrated guided mode filters (CRIGFs; Section 5.7.2) and as external cavity mirrors (Section 5.7.3).

5.7.1. Intra-Cavity Mirrors and Distributed Feedback Lasers

RWG mirrors can be designed to achieve a narrower linewidth and higher polarization selectivity[339–341] compared to conventional narrowband mirrors, such as Fabry–Perot cavities. Moreover, they also provide lower thermal noise and lower mechanical losses thanks to their lower overall thickness.[56,342] For this reason, RWG cavity mirrors have been, for example, implemented in advanced gravitational wave detectors, where the main source of noise is the cavities mirrors.[343–345] Several configurations of RWG cavity mirrors have been reported, such as silicon on silica T-like structures,[57] monolithic single silicon crystal mirrors (as illustrated in **Figure 17**a,b)[346] and stacks of multiple RWGs (Figure 17c).[193,347] RWGs can be also be used as distributed feedback resonators in combination with planar organic thin films to engineer lasers which are more compact and easier to integrate.[165,348]

5.7.2. Cavity Resonator Integrated Guided Mode Resonance Filters

CRIGFs consist of a coupling grating filter fabricated between two DBRs, as sketched in **Figure 18**a. A wave vertically injected to the CRIGF is coupled by the grating to guided waves propagating contra-directionally with each other. The excited guided waves are reflected by the DBRs when reaching the end of the cavity, and can also be coupled out by the same grating coupler to radiation waves. The radiation waves are superimposed to the directly transmitted and reflected waves. When the reflectance of both DBRs is 100%, the guided wave power is accumulated enough to cancel the direct transmission or reflection. This particular configuration provides a high wavelength selectivity even with small (micrometer-size) apertures, whilst preserving a high angular acceptance.[349,350] CRIGFs were first developed to have high-efficiency coupling[289,351] before being implemented as filters working with a miniaturized aperture size.[352,353] The relative position between the coupling grating and the DBRs, the cavity length[354,355] as well as the waveguide thickness,[356] have to be properly tuned for phase adjustment of the waves resulting from out-coupling of the forward and backward guided waves. More advanced concepts have been developed for the DBRs

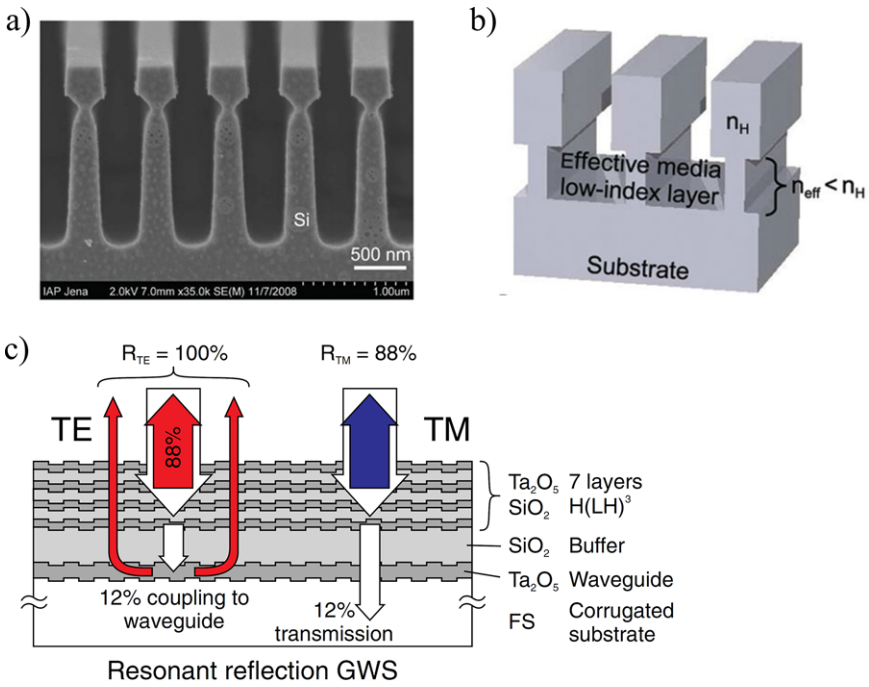

Figure 17. a) Scanning electron microscope image and b) schematic of a monolithic cavity mirror. Reproduced with permission.[346] Copyright 2012, American Physical Society. c) Schematic of an intra-cavity mirror made with multiple layers for the generation of azimuthal polarized beams. Reproduced with permission.[193] Copyright 2012, Optical Society of America.

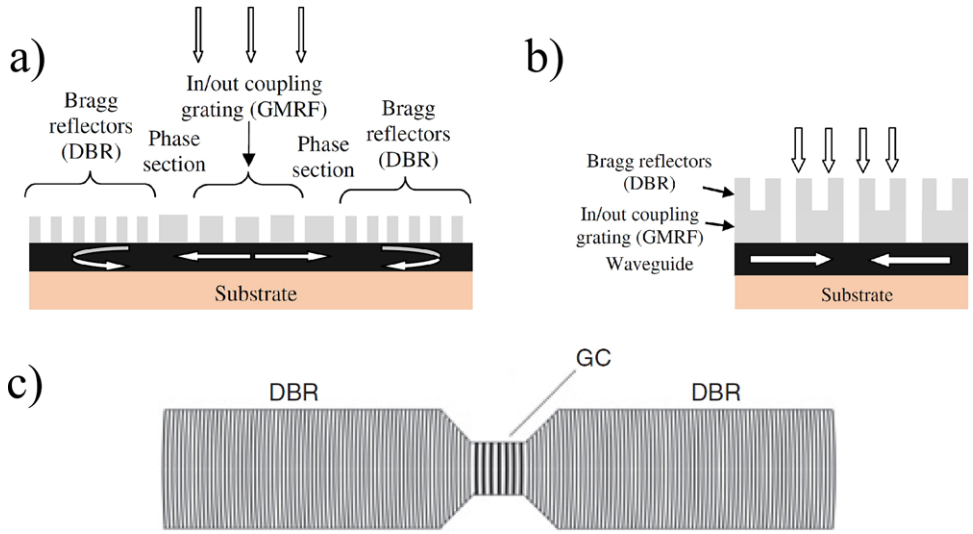

Figure 18. a) Schematic of a CRIGF. b) CRIGF with the superposition of DBR and coupling grating. Reproduced with permission.[350] Copyright 2015, OSA. c) CRIGF with circular DBRs. Reproduced with permission.[192] Copyright 2012, The Institution of Engineering and Technology.

and the RWG in order to obtain specific optical responses. The analysis in terms of 1D and 2D photonic crystal heterostructures has been studied by Sciancalepore et al.[357,358] In particular, they proposed a structure consisting of three different adjacent photonic crystals, in which photons can only propagate in the central pass-band crystal because of a forbidden bandgap region in the side crystals. Furthermore, the structure can be utilized for both the top and the bottom reflectors. DBRs can be designed with curved gratings to better reflect the diverging guided waves (see Figure 18c)[192] or they can be superimposed onto the coupling grating as in Figure 18b, while non-uniform RWGs allows to efficiently couple Gaussian beams.[359] Other features include the integration of two orthogonally crossed CRIGFs exhibits polarization-independent reflectance spectra.[360] A high-reflection layer can be added to have high reflectance and large phase variations for a subnanometer wavelength shift.[361] Analytical and numerical models have been proposed for efficiently designing such new filters.[362–364]

5.7.3. External Cavity Mirrors

For many applications such as absorption spectroscopy or optical communications, it is necessary to have a single frequency laser together with the possibility to adjust the lasing wavelength by means of external lasing mirrors.[365] Avrutskii et al. were the first to control the emission of a dye layer with a single mode RWG;[22,25] further works were carried out with semiconductor lasers.[366,367] Further works show progress in the design in order to achieve specific optical properties. A steep π-phase variation combined with high reflectance over a small wavelength interval of 10 nm in the mid-IR has been shown using an RWG.[368] By symmetry, 2D configurations can provide polarization insensitivity in the reflection band.[369] A spatial modulation of the structure parameters provide frequency-dependent spatial reflection and transmission of the beam profile.[370] External laser cavities can be used to combine the emission of multiple laser diodes,[371] to improve the emission and the quality factor in short-cavity laser diodes,[372] or in optical fiber lasers.[373,374]

5.8. Optical Security

In the early 1980s the fraction of counterfeited US dollars and other major currencies experienced a rise due to the widespread accessibility of new low-cost printing technologies, that is, photocopiers and color photocopiers. This driving force and the invention of very high-throughput and affordable production techniques based on roll-to-roll NIL and PVD enabled the wide implementation of optically variable devices (OVDs) and their use to secured various documents and goods such as credit cards, banknotes, and identification documents.[375] Following the successful implementation of diffractive optically variable image devices (DOVIDs), RWGs-based diffractive identification devices (DID) demonstrated a particularly high robustness against forging[376] and enable visual control in any light condition, including fully diffused ambient lighting thanks to a color-angular-dependent zero-order reflection.[53] The working principle builds on highly corrugated waveguide geometries having a broadband reflection in the visible spectral range. The angular dependency of the zero-order specular reflection give rise to various color perceptions at different observation points. Authentication labels made with RWGs work under unpolarized white light, are polarization dependent and are easily distinguishable under particular viewing angles by naked eyes while maintaining a high transparency.[377] In particular, a maximal visual impact has been reached with a green to red color inversion when rotating the observation point from collinear (i.e., across grating lines) to conical (i.e., along grating lines) at an oblique viewing angle located approximately at 30° from the normal to the document. RWGs are currently used to secure billions of documents every year including identification documents in the form of security overlays on passport data pages and identity cards[378] (example in **Figure 19**a). Since the first implementation on passport in 2003, not a single counterfeiting or lure of the DID could be reported despite their use in more than 40 countries. Various new developments and variations allow designing different control protocols and viewing angles (Figure 19b)[379] or control using readers such as smartphones (Figure 19c).[116]

6. Conclusion and Outlook

RWGs, also known as guided mode resonances (GMRs) and many different appellations, use the periodicity of a grating to couple light into a thin waveguide. They have been therefore used extensively as waveguide couplers for optical communication and signal processing for the in-coupling and out-coupling of thin waveguide modes with strong wavelength, polarization, and angular dependences. Their in-coupled quasi-guided modes can interfere dramatically with the incident illumination depending on the phase delay accumulated in the in-coupling in the waveguide which create anomalous reflection and transmission features, creating unique zeroth-order properties. This mechanism makes them highly efficient narrowband or broadband reflectors, as well as transmission filters with applications as laser mirrors, advanced detection systems, or spectrometers as well as highly efficient diffraction element off the Littrow configuration. In another direction, cost-efficient fabrication processes and unique appearance have enabled their pervasive use as OVDs in optical authentication and document security. Their polarization-dependent behavior has led to the development of polarizers, polarization rotators, and wave plates. The control of the optical near-field has found widespread applications in biological refractive index sensing, fluorescence sensing, nonlinear effects, and optical switching, as well has enhancement of solar light harvesting.

Dedicated numerical methods have been developed and optimized for their design, including the RCWA, the C-method, or integral methods. Popular numerical algorithms such as FDTD or finite elements have also been used, and new analytical methods and fitting have also been suggested, for example, by modeling Feshbach resonances.[380] The increase of computational power together with method optimizations and optimization algorithms is expected to enable the design of increasingly complex and realistic devices, closer to fabrication and industrial implementation.[381] Fabrication methods based on laser interference lithography directly and efficiently produce the required periodic microscale or nanoscale patterns, while more versatile methods such as electron beam lithography have also been used. Replication and fabrication techniques have allowed higher throughput, lower cost, and better accuracy fabrication for both research and development and industrial production.

The polarization, phase, and intensity of an optical field can be tailored using RWGs, which has led to further implementations, for example, as focusing elements. Combination with other optical structures or resonators has opened a variety of optical functionalities and enhancement of their efficiency. Recent research on the active control of RWGs by mechanical (MOEMS, NOEMS), electrical (liquid crystals), or thermal means has also set the path for further opportunities. The implementation of such complex RWGs now calls for efficient design and fabrication methods in order to enable their transfer toward the photonics industry. Thanks to these developments in mastering nanostructures and benefitting from established large throughput replication processes, RWGs are promising building blocks for other emerging paradigms, such as wavefront control and light routing metasurfaces[382] with high coupling and small confinement between different unit cells. RWG properties can be used as well on 2D structures to make photonic crystals

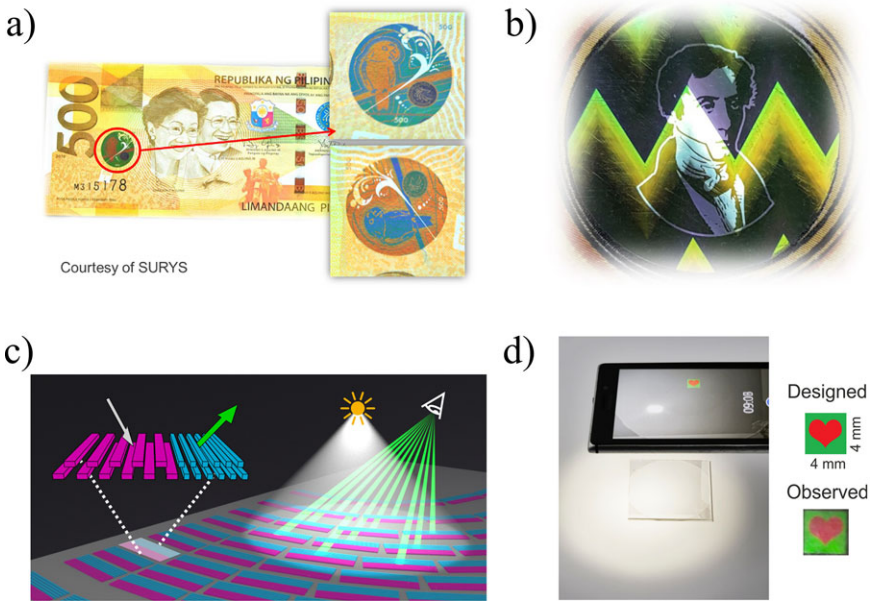

Figure 19. a) DID patch produced by Surys and securing the large denomination banknotes of the Philippines where reflective color permutation is achieved for a 90° document rotation. b) DID Graphic Wave security label providing out of specular visibility and dynamic graphics. Reproduced with permission.[379] Copyright 2017, Surys. c) Sketch and d) photo of a realization as security label for smartphone authentication. Reproduced with permission.[116] Copyright 2017, American Chemical Society.

relying on leaky guided modes as analyzed by Fan[383] or used by Wang[384] and Matsui.[385] Finally, the delocalized horizontal GMR of RWG can be used in synergy with other photonic elements, resonant or not, or rely on new materials such as 2D materials.[386] An understanding of the complex nature of the materials together with the established knowledge on the physics of quasi-guided modes is expected to open new avenues of research. The broad range of unique properties of RWGs and their ease of fabrication calls for new exciting research, development, and industrial applications in the future.

Conflict of Interest

The authors declare no conflict of interest.

Keywords

corrugated waveguides, grating couplers, guided mode resonances, leaky mode resonances, resonant waveguide gratings

Received: January 19, 2018
Revised: June 11, 2018
Published online: July 30, 2018

[1] R. W. Wood, *Proc. Phys. Soc. Lond.* **1902**, *18*, 269.
[2] Lord Rayleigh, *Proc. R. Soc. Lond. Ser. Contain. Pap. Math. Phys. Character* **1907**, *79*, 399.
[3] U. Fano, *JOSA* **1941**, *31*, 213.
[4] A. Hessel, A. A. Oliner, *Appl. Opt.* **1965**, *4*, 1275.
[5] D. Maystre, *Opt. Commun.* **1972**, *6*, 50.
[6] P. Lalanne, J. P. Hugonin, P. Chavel, *J. Light. Technol.* **2006**, *24*, 2442.
[7] C. J. Chang-Hasnain, W. Yang, *Adv. Opt. Photonics* **2012**, *4*, 379.
[8] K. Knop, *JOSA* **1978**, *68*, 1206.
[9] M. L. Dakss, L. Kuhn, P. F. Heidrich, B. A. Scott, *Appl. Phys. Lett.* **1970**, *16*, 523.
[10] H. Kogelnik, T. P. Sosnowski, *Bell Syst. Tech. J.* **1970**, *49*, 1602.
[11] H. Kogelnik, C. V. Shank, *J. Appl. Phys.* **1972**, *43*, 2327.
[12] S. Wang, *IEEE J. Quantum Electron.* **1974**, *10*, 413.
[13] D. B. Ostrowsky, A. Jacques, *Appl. Phys. Lett.* **1971**, *18*, 556.
[14] M. Neviere, R. Petit, M. Cadilhac, *Opt. Commun.* **1973**, *8*, 113.
[15] M. Neviere, P. Vincent, R. Petit, M. Cadilhac, *Opt. Commun.* **1973**, *9*, 48.
[16] M. Neviere, P. Vincent, R. Petit, M. Cadilhac, *Opt. Commun.* **1973**, *9*, 240.
[17] A. Jacques, D. B. Ostrowsky, *Opt. Commun.* **1975**, *13*, 74.
[18] K. Knop, R. Morf, *WO8300395 (A1)*, **1983**.
[19] V. A. Sychugov, A. V. Tishchenko, *Sov. J. Quantum Electron.* **1980**, *10*, 186.
[20] V. A. Sychugov, A. V. Tishchenko, *Sov. J. Quantum Electron.* **1982**, *12*, 923.
[21] G. A. Golubenko, A. S. Svakhin, V. A. Sychugov, A. V. Tishchenko, *Sov. J. Quantum Electron.* **1985**, *15*, 886.
[22] I. D. Avrutskii, G. A. Golubenko, V. A. Sychugov, A. V. Tishchenko, *Tech. Phys. Lett.* **1985**, *11*, 971.
[23] L. Mashev, E. Popov, *Opt. Commun.* **1984**, *51*, 131.
[24] L. Mashev, E. Popov, *Opt. Commun.* **1985**, *55*, 377.
[25] I. A. Avrutskiĭ, G. A. Golubenko, V. A. Sychugov, A. V. Tishchenko, *Sov. J. Quantum Electron.* **1986**, *16*, 1063.
[26] G. A. Golubenko, A. S. Svakhin, V. A. Sychugov, A. V. Tischenko, E. Popov, L. Mashev, *Opt. Quantum Electron.* **1986**, *18*, 123.
[27] I. A. Avrutsky, V. A. Sychugov, *J. Mod. Opt.* **1989**, *36*, 1527.
[28] T. Tamir (Ed.), *Integrated Optics*, Springer, Berlin **1975**.
[29] R. Petit (Ed.), *Electromagnetic Theory of Gratings*, Springer, Berlin **1980**.
[30] D. Rosenblatt, A. Sharon, A. A. Friesem, *IEEE J. Quantum Electron.* **1997**, *33*, 2038.

[31] R. Magnusson, Y. Ding, K. J. Lee, D. Shin, P. S. Priambodo, P. P. Young, T. A. Maldonado, in International Society for Optics and Photonics, Optical Science and Technology, SPIE's 48th Annual Meeting, **2003**, San Diego, California, United States (https://doi.org/10.1117/12.504425), 20.
[32] R. Magnusson, M. Shokooh-Saremi, K. J. Lee, J. Curzan, D. Wawro, S. Zimmerman, W. Wu, J. Yoon, H. G. Svavarsson, S. H. Song, in (Eds: E. A. Dobisz, L. A. Eldada), SPIE NanoScience + Engineering, **2011**, San Diego, California, United States (https://doi.org/10.1117/12.896431), 810202.
[33] R. Magnusson, J. W. Yoon, M. S. Amin, T. Khaleque, M. J. Uddin, in (Eds: J. E. Broquin, G. Nunzi Conti), SPIE OPTO, **2014**, San Francisco, California, United States (https://doi.org/10.1117/12.2039729), 89880I.
[34] R. Magnusson, Y. H. Ko, in (Eds: E. M. Campo, E. A. Dobisz, L. A. Eldada), SPIE Nanoscience + Engineering, **2016**, San Diego, California, United States (https://doi.org/10.1117/12.2237973), 992702.
[35] R. Magnusson, M. Niraula, J. W. Yoon, Y. H. Ko, K. J. Lee, in (Eds: C. J. Chang-Hasnain, D. Fattal, F. Koyama, W. Zhou), SPIE OPTO, **2016**, San Francisco, California, United States (https://doi.org/10.1117/12.2211687), 975705.
[36] M. A. Cooper, *Drug Discov. Today* **2006**, *11*, 1061.
[37] Y. Fang, *ASSAY Drug Dev. Technol.* **2006**, *4*, 583.
[38] D. Wawro, S. Tibuleac, R. Magnusson, *Optical Imaging Sensors and Systems For Homeland Security Applications*, Springer, New York **2006**, 367.
[39] I. Abdulhalim, in *Optical Waveguide Sensing and Imaging*, Springer, Dordrecht **2008**, 211.
[40] K. Erdélyi, A. G. Frutos, J. J. Ramsden, I. Szendrő, G. Voirin, *Handbook of Biosensors and Biochips*, John Wiley & Sons Ltd, New York **2008**.
[41] Y. Fang, A. G. Frutos, R. Verklereen, *Comb. Chem. High Throughput Screen.* **2008**, *11*, 357.
[42] Y. Fang, A. M. Ferrie, E. Tran, *G Protein-Coupled Receptors in Drug Discovery*, Humana Press, Totowa, NJ **2009**, 239.
[43] F. Pröll, P. Fechner, G. Proll, *Anal. Bioanal. Chem.* **2009**, *393*, 1557.
[44] K. Schmitt, C. Hoffmann, in *Optical Guided-Wave Chemical and Biosensors*, (Eds: I. M. Zourob, A. Lakhtakia), Springer, Berlin **2010**, 21.
[45] H. N. Daghestani, B. W. Day, *Sensors* **2010**, *10*, 9630.
[46] S. Geschwindner, J. F. Carlsson, W. Knecht, *Sensors* **2012**, *12*, 4311.
[47] R. Halai, M. A. Cooper, *Expert Opin. Drug Discov.* **2012**, *7*, 123.
[48] A. Fernández Gavela, D. Grajales García, J. Ramirez, L. Lechuga, *Sensors* **2016**, *16*, 285.
[49] M. Paulsen, S. Jahns, M. Gerken, *Photonics Nanostructures Fundam. Appl.* **2017**, *26*, 69.
[50] R. Halir, P. J. Bock, P. Cheben, A. Ortega-Moñux, C. Alonso-Ramos, J. H. Schmid, J. Lapointe, D.-X. Xu, J. G. Wangüemert-Pérez, Í. Molina-Fernández, S. Janz, *Laser Photonics Rev.* **2015**, *9*, 25.
[51] P. Qiao, W. Yang, C. J. Chang-Hasnain, *ArXiv Prepr.* **2017**, ArXiv170707753.
[52] A.-L. Fehrembach, A. Talneau, O. Boyko, F. Lemarchand, A. Sentenac, *Opt. Lett.* **2007**, *32*, 2269.
[53] M. T. Gale, K. Knop, R. H. Morf, in: International Society for Optics and Photonics, OE/LASE '90, **1990**, Los Angeles, CA, United States (https://doi.org/10.1117/12.17917), 83.
[54] S. Tibuleac, R. Magnusson, *JOSA A* **1997**, *14*, 1617.
[55] N. Destouches, A. V. Tishchenko, J. C. Pommier, S. Reynaud, O. Parriaux, S. Tonchev, M. A. Ahmed, *Opt. Express* **2005**, *13*, 3230.
[56] M. Rumpel, B. Dannecker, A. Voss, M. Moeller, C. Moormann, T. Graf, M. A. Ahmed, *Opt. Lett.* **2013**, *38*, 4766.
[57] S. Kroker, T. Käsebier, F. Brückner, F. Fuchs, E.-B. Kley, A. Tünnermann, *Opt. Express* **2011**, *19*, 16466.
[58] N. V. Golovastikov, D. A. Bykov, L. L. Doskolovich, *Quantum Electron.* **2014**, *44*, 984.
[59] M. Neviere, E. Popov, R. Reinisch, G. Vitrant, *Electromagnetic Resonances in Nonlinear Optics*, CRC Press, London **2000**.
[60] S. S. Wang, R. Magnusson, *Appl. Opt.* **1993**, *32*, 2606.
[61] D. Shin, S. Tibuleac, T. A. Maldonado, R. Magnusson, *Opt. Eng.* **1998**, *37*, 2634.
[62] P. Lalanne, D. Lemercier-lalanne, *J. Mod. Opt.* **1996**, *43*, 2063.
[63] D. L. Brundrett, E. N. Glytsis, T. K. Gaylord, J. M. Bendickson, *JOSA A* **2000**, *17*, 1221.
[64] K. Han, C.-H. Chang, *Nanomaterials* **2014**, *4*, 87.
[65] D. L. Brundrett, E. N. Glytsis, T. K. Gaylord, *Appl. Opt.* **1996**, *35*, 6195.
[66] C. Forestiere, A. J. Pasquale, A. Capretti, G. Miano, A. Tamburrino, S. Y. Lee, B. M. Reinhard, L. Dal Negro, *Nano Lett.* **2012**, *12*, 2037.
[67] M. Imran, R. Hashim, N. E. A. Khalid, *Procedia Eng.* **2013**, *53*, 491.
[68] M. G. Moharam, E. B. Grann, D. A. Pommet, T. K. Gaylord, *JOSA A* **1995**, *12*, 1068.
[69] M. G. Moharam, D. A. Pommet, E. B. Grann, T. K. Gaylord, *JOSA A* **1995**, *12*, 1077.
[70] G. Granet, B. Guizal, *JOSA A* **1996**, *13*, 1019.
[71] P. Lalanne, G. M. Morris, *JOSA A* **1996**, *13*, 779.
[72] L. Li, *JOSA A* **1996**, *13*, 1870.
[73] N. M. Lyndin, O. Parriaux, A. V. Tishchenko, *JOSA A* **2007**, *24*, 3781.
[74] N. L. Kazanskiy, P. G. Serafimovich, *Adv. Opt. Technol.* **2012**, 1.
[75] M. Pisarenco, I. D. Setija, *J. Comput. Phys.* **2014**, *261*, 130.
[76] B. Guizal, D. Barchiesi, D. Felbacq, *JOSA A* **2003**, *20*, 2274.
[77] P. Lalanne, E. Silberstein, *Opt. Lett.* **2000**, *25*, 1092.
[78] G. Lecamp, J. P. Hugonin, P. Lalanne, *Opt. Express* **2007**, *15*, 11042.
[79] J. Chandezon, G. Raoult, D. Maystre, *J. Opt.* **1980**, *11*, 235.
[80] J. Chandezon, M. T. Dupuis, G. Cornet, D. Maystre, *JOSA* **1982**, *72*, 839.
[81] T. W. Preist, N. P. K. Cotter, J. R. Sambles, *JOSA A* **1995**, *12*, 1740.
[82] L. Li, J. Chandezon, *JOSA A* **1996**, *13*, 2247.
[83] T. Vallius, *JOSA A* **2002**, *19*, 1555.
[84] B. T. Draine, P. J. Flatau, *JOSA A* **1994**, *11*, 1491.
[85] B. T. Draine, *Astrophys. J.* **1988**, *333*, 848.
[86] P. C. Chaumet, A. Rahmani, G. W. Bryant, *Phys. Rev. B* **2003**, *67*, 165404.
[87] P. C. Chaumet, A. Sentenac, *Phys. Rev. B* **2005**, *72*, 205437.
[88] P. C. Chaumet, A. Sentenac, *J. Quant. Spectrosc. Radiat. Transf.* **2009**, *110*, 409.
[89] B. Gallinet, J. Butet, O. J. F. Martin, *Laser Photonics Rev.* **2015**, *9*, 577.
[90] M. Paulus, O. J. F. Martin, *Phys. Rev. E* **2001**, *63*, 066615.
[91] M. Paulus, O. J. F. Martin, *JOSA A* **2001**, *18*, 854.
[92] G. Lévêque, O. J. F. Martin, *J. Appl. Phys.* **2006**, *100*, 124301.
[93] N. L. Tsitsas, N. K. Uzunoglu, D. I. Kaklamani, *Radio Sci.* **2007**, *42*.
[94] R. F. Harrington, *Field Computation by Moment Methods*, Macmillan, New York **1968**.
[95] N. Marly, D. D. Zutter, H. F. Pues, *IEEE Trans. Electromagn. Compat.* **1994**, *36*, 14.
[96] B. Gallinet, A. M. Kern, O. J. F. Martin, *JOSA A* **2010**, *27*, 2261.
[97] M. Paulus, P. Gay-Balmaz, O. J. F. Martin, *Phys. Rev. E* **2000**, *62*, 5797.
[98] A. Taflove, S. C. Hagness, *Computational Electrodynamics: The Finite-Difference Time-Domain Method*, Artech House, Boston, MA **2005**.
[99] B. Liang, M. Bai, H. Ma, N. Ou, J. Miao, *IEEE Trans. Antennas Propag.* **2014**, *62*, 354.
[100] J. Jin, *The Finite Element Method in Electromagnetics*, 3rd ed. Wiley-IEEE Press, Hoboken, NJ **2014**.
[101] K. Busch, M. König, J. Niegemann, *Laser Photonics Rev.* **2011**, *5*, 773.
[102] M. V. Shuba, A. Lakhtakia, *JOSA A* **2016**, *33*, 779.
[103] H. P. Herzig, *Micro-Optics: Elements, Systems and Applications*, CRC Press, London **1997**.

[104] M. J. Madou, *Manufacturing Techniques for Microfabrication and Nanotechnology*, CRC Press, Boca Raton, FL **2011**.
[105] K. J. Gåsvik, *Optical Metrology*, John Wiley & Sons, Hoboken, NJ **2003**.
[106] T. Yoshizawa, *Handbook of Optical Metrology: Principles and Applications*, CRC Press, Boca Raton, FL **2009**.
[107] C. Lu, R. h. Lipson, *Laser Photonics Rev*. **2010**, *4*, 568.
[108] H. H. Solak, C. David, J. Gobrecht, V. Golovkina, F. Cerrina, S. O. Kim, P. F. Nealey, *Microelectron. Eng.* **2003**, *67–68*, 56.
[109] C. Vieu, F. Carcenac, A. Pépin, Y. Chen, M. Mejias, A. Lebib, L. Manin-Ferlazzo, L. Couraud, H. Launois, *Appl. Surf. Sci.* **2000**, *164*, 111.
[110] M. Paulsen, L. T. Neustock, S. Jahns, J. Adam, M. Gerken, *Opt. Quantum Electron.* **2017**, *49*, 107.
[111] N. Eriksson, M. Hagberg, A. Larsson, *J. Vac. Sci. Technol. B Microelectron. Nanometer Struct. Process. Meas. Phenom.* **1996**, *14*, 184.
[112] W. W. Hu, K. Sarveswaran, M. Lieberman, G. H. Bernstein, *J. Vac. Sci. Technol. B Microelectron. Nanometer Struct. Process. Meas. Phenom.* **2004**, *22*, 1711.
[113] A. E. Grigorescu, C. W. Hagen, *Nanotechnology* **2009**, *20*, 292001.
[114] A. Talneau, F. Lemarchand, A.-L. Fehrembach, A. Sentenac, *Appl. Opt.* **2010**, *49*, 658.
[115] K. Li, J. Li, C. Reardon, C. S. Schuster, Y. Wang, G. J. Triggs, N. Damnik, J. Müenchenberger, X. Wang, E. R. Martins, T. F. Krauss, *Sci. Rep.* **2016**, *6*, 32945.
[116] G. Quaranta, G. Basset, O. J. F. Martin, B. Gallinet, *ACS Photonics* **2017**, *4*, 1060.
[117] S. Singh, M. Argument, Y. Y. Tsui, R. Fedosejevs, *J. Appl. Phys.* **2005**, *98*, 113520.
[118] M. A. Bader, C. Kappel, A. Selle, J. Ihlemann, M. L. Ng, P. R. Herman, *Appl. Opt.* **2006**, *45*, 6586.
[119] J. Bekesi, J. Meinertz, J. Ihlemann, P. Simon, *Appl. Phys. A* **2008**, *93*, 27.
[120] R. C. Rumpf, E. G. Johnson, *Opt. Express* **2007**, *15*, 3452.
[121] J. Wang, Q. Wang, Y. Li, P. Chen, T. Huang, B. Dai, Y. Huang, D. Zhang, *J. Opt.* **2016**, *45*, 302.
[122] Q. Wang, D. Zhang, H. He, Y. Huang, J. Chen, L. Chen, Y. Zhu, S. Zhuang, *Opt. Lett.* **2009**, *34*, 70.
[123] M. R. Saleem, S. Honkanen, J. Turunen, *Appl. Opt.* **2013**, *52*, 422.
[124] M. Scobey, P. Egerton, R. Fortenberry, *SPIE Newsroom*, http://doi.org/10.1117/2.1201312.005269 (18 December **2013**).
[125] M. R. Saleem, R. Ali, M. B. Khan, S. Honkanen, J. Turunen, *Front. Mater.* **2014**, *1*, 1.
[126] D. W. Dobbs, I. Gershkovich, B. T. Cunningham, *Appl. Phys. Lett.* **2006**, *89*, 123113.
[127] Y. Nazirizadeh, F. von Oertzen, T. Karrock, J. Greve, M. Gerken, *Opt. Express* **2013**, *21*, 18661.
[128] S. Y. Chou, P. R. Krauss, P. J. Renstrom, *Appl. Phys. Lett.* **1995**, *67*, 3114.
[129] H. Schift, P. Urwyler, P. M. Kristiansen, J. Gobrecht, *J. MicroNanolithography MEMS MOEMS* **2014**, *13*, 031303.
[130] M. T. Gale, *Microelectron. Eng.* **1997**, *34*, 321.
[131] P. Reader-Harris, A. Ricciardi, T. Krauss, A. D. Falco, *Opt. Express* **2013**, *21*, 1002.
[132] V. K. Parashar, A. Sayah, M. Pfeffer, F. Schoch, J. Gobrecht, M. A. M. Gijs, *Microelectron. Eng.* **2003**, *67*-68, 710.
[133] K. J. Lee, J. Jin, B.-S. Bae, R. Magnusson, *Opt. Lett.* **2009**, *34*, 2510.
[134] Y. Nazirizadeh, F. von Oertzen, K. Plewa, N. Barié, P.-J. Jakobs, M. Guttmann, H. Leiste, M. Gerken, *Opt. Mater. Express* **2013**, *3*, 556.
[135] M. D. Fagan, B. H. Kim, D. Yao, *Adv. Polym. Technol.* **2009**, *28*, 246.
[136] L. Davoine, V. Paeder, G. Basset, M. Schnieper, H. P. Herzig, *Appl. Opt.* **2013**, *52*, 340.
[137] G. Quaranta, G. Basset, O. J. F. Martin, B. Gallinet, in International Society for Optics and Photonics, SPIE Nanoscience + Engineering, **2017**, San Diego, California, United States (https://doi.org/10.1117/12.2272683), 1035408.
[138] T. Khaleque, H. G. Svavarsson, R. Magnusson, *Opt. Express* **2013**, *21*, A631.
[139] L. Liu, J. Zhang, M. A. Badshah, L. Dong, J. Li, S. Kim, M. Lu, *Sci. Rep.* **2016**, *6*, 22445.
[140] M. Qian, W. Zhang, D. Trefilov, M. Ji, Y. Cui, C. Yuan, W. Li, H. Ge, Y. Chen, *Appl. Phys. A* **2016**, *122*, 577.
[141] W.-K. Kuo, Y.-M. Chang, *Appl. Opt.* **2017**, *56*, 99.
[142] Y. Huang, L. Liu, M. Johnson, A. C Hillier, M. Lu, *Nanotechnology* **2016**, *27*, 095302.
[143] M. R. Saleem, D. Zheng, B. Bai, P. Stenberg, M. Kuittinen, S. Honkanen, J. Turunen, *Opt. Express* **2012**, *20*, 16974.
[144] G. Niederer, H. P. Herzig, J. Shamir, H. Thiele, M. Schnieper, C. Zschokke, *Appl. Opt.* **2004**, *43*, 1683.
[145] C. F. R. Mateus, M. C. Y. Huang, Y. Deng, A. R. Neureuther, C. J. Chang-Hasnain, *IEEE Photonics Technol. Lett.* **2004**, *16*, 518.
[146] A. Ricciardi, S. Campopiano, A. Cusano, T. F. Krauss, L. O'Faolain, *IEEE Photonics J*. **2010**, *2*, 696.
[147] K. Bougot-Robin, W. Wen, H. Benisty, *Biomed. Opt. Express* **2012**, *3*, 2436.
[148] G. Zheng, L. Zhao, L. Qian, F. Xian, L. Xu, *Opt. Commun.* **2016**, *358*, 140.
[149] D. A. Bykov, L. L. Doskolovich, V. A. Soifer, *Opt. Express* **2017**, *25*, 1151.
[150] E. Popov, L. Mashev, D. Maystre, *Opt. Acta Int. J. Opt.* **1986**, *33*, 607.
[151] A.-L. Fehrembach, K. Sharshavina, F. Lemarchand, E. Popov, A. Monmayrant, P. Arguel, O. Gauthier-Lafaye, *JOSA A* **2017**, *34*, 234.
[152] M. Niraula, J. W. Yoon, R. Magnusson, *Opt. Express* **2014**, *22*, 25817.
[153] M. Niraula, J. W. Yoon, R. Magnusson, *Opt. Express* **2015**, *23*, 23428.
[154] T. Khaleque, M. J. Uddin, R. Magnusson, *Opt. Express* **2014**, *22*, 12349.
[155] R. Magnusson, *Opt. Lett.* **2014**, *39*, 4337.
[156] W. Yu, D. Wu, X. Duan, Y. Yi, *MRS Adv*. **2016**, *1*, 1683.
[157] R. Magnusson, *Opt. Lett.* **2013**, *38*, 989.
[158] M. Shyiq Amin, J. Woong Yoon, R. Magnusson, *Appl. Phys. Lett.* **2013**, *103*, 131106.
[159] D. Maystre, in *Plasmonics*, (Eds: S. Enoch, N. Bonod), Springer, Berlin **2012**, 39.
[160] A. T. M. A. Rahman, P. Majewski, K. Vasilev, *Opt. Lett.* **2012**, *37*, 1742.
[161] L. Qian, D. Zhang, C. Tao, R. Hong, S. Zhuang, *Opt. Lett.* **2016**, *41*, 982.
[162] M.-L. Wu, C.-L. Hsu, Y.-C. Liu, C.-M. Wang, J.-Y. Chang, *Opt. Lett.* **2006**, *31*, 3333.
[163] Y.-L. Tsai, J.-Y. Chang, M.-L. Wu, Z.-R. Tu, C.-C. Lee, C.-M. Wang, C.-L. Hsu, *Opt. Lett.* **2010**, *35*, 4199.
[164] C.-C. Chang, H.-C. Lan, H.-L. Hsiao, J.-W. Jheng, I.-C. Lu, Y.-C. Lee, M.-L. Wu, *Jpn. J. Appl. Phys.* **2010**, *49*, 052202.
[165] N. Matsuyama, Y. Kanamori, J.-S. Ye, K. Hane, *J. Opt. Pure Appl. Opt.* **2007**, *9*, 940.
[166] A. T. Cannistra, M. K. Poutous, E. G. Johnson, T. J. Suleski, *Opt. Lett.* **2011**, *36*, 1155.
[167] J. Ma, S. Liu, D. Zhang, J. Yao, C. Xu, J. Shao, Y. Jin, Z. Fan, *J. Opt. Pure Appl. Opt.* **2008**, *10*, 025302.
[168] O. Stenzel, S. Wilbrandt, X. Chen, R. Schlegel, L. Coriand, A. Duparré, U. Zeitner, T. Benkenstein, C. Wächter, *Appl. Opt.* **2014**, *53*, 3147.
[169] J. P. Kottmann, O. J. F. Martin, D. R. Smith, S. Schultz, *Phys. Rev. B* **2001**, *64*, 235402.
[170] O. Parriaux, G. Voirin, *Sens. Actuators Phys.* **1990**, *23*, 1137.
[171] T. Siegfried, L. Wang, Y. Ekinci, O. J. F. Martin, H. Sigg, *ACS Nano* **2014**, *8*, 3700.
[172] D. B. Mazulquim, K. J. Lee, J. W. Yoon, L. V. Muniz, B.-H. V. Borges, L. G. Neto, R. Magnusson, *Opt. Express* **2014**, *22*, 30843.

[173] D. Mazulquim, K. J. Lee, L. V. Muniz, B.-H. V. Borges, L. G. Neto, R. Magnusson, in *Frontiers in Optics 2014*, Optical Society of America **2014**, FTh3D.7.
[174] I. Koirala, V. R. Shrestha, C.-S. Park, S.-S. Lee, D.-Y. Choi, *Sci. Rep.* **2017**, *7*, 40073.
[175] N. Nguyen-Huu, Y.-L. Lo, Y.-B. Chen, *Opt. Commun.* **2011**, *284*, 2473.
[176] J. Wang, Q. Fan, S. Zhang, Z. Zhang, H. Zhang, Y. Liang, X. Cao, T. Xu, *Appl. Phys. Lett.* **2017**, *110*, 031110.
[177] H.-T. Chen, A. J. Taylor, N. Yu, *Rep. Prog. Phys.* **2016**, *79*, 076401.
[178] Z. Li, M.-H. Kim, C. Wang, Z. Han, S. Shrestha, A. C. Overvig, M. Lu, A. Stein, A. M. Agarwal, M. Lončar, N. Yu, *Nat. Nanotechnol.* **2017**, *12*, 675.
[179] C.-H. Park, Y.-T. Yoon, V. R. Shrestha, C.-S. Park, S.-S. Lee, E.-S. Kim, *Opt. Express* **2013**, *21*, 28783.
[180] J. Homola, *Anal. Bioanal. Chem.* **2003**, *377*, 528.
[181] R. Magnusson, J. Yoon, D. Wawro, in (Eds: B. L. Miller, P. M. Fauchet) **2013**, 85700K.
[182] F.-C. Chien, C.-Y. Lin, J.-N. Yih, K.-L. Lee, C.-W. Chang, P.-K. Wei, C.-C. Sun, S.-J. Chen, *Biosens. Bioelectron.* **2007**, *22*, 2737.
[183] P. Zeng, J. Cadusch, D. Chakraborty, T. A. Smith, A. Roberts, J. E. Sader, T. J. Davis, D. E. Gómez, *Nano Lett.* **2016**, *16*, 2651.
[184] W. L. Barnes, A. Dereux, T. W. Ebbesen, *Nature* **2003**, *424*, 824.
[185] F. López-Tejeira, S. G. Rodrigo, L. Martín-Moreno, F. J. García-Vidal, E. Devaux, T. W. Ebbesen, J. R. Krenn, I. P. Radko, S. I. Bozhevolnyi, M. U. González, J. C. Weeber, A. Dereux, *Nat. Phys.* **2007**, *3*, 324.
[186] E. Devaux, T. W. Ebbesen, J.-C. Weeber, A. Dereux, *Appl. Phys. Lett.* **2003**, *83*, 4936.
[187] P. K. Tien, *Opt. Lett.* **1977**, *1*, 64.
[188] D. Heitmann, C. Ortiz, *IEEE J. Quantum Electron.* **1981**, *17*, 1257.
[189] S. Nishiwaki, J. Asada, S. Uchida, *Appl. Opt.* **1994**, *33*, 1819.
[190] K. Kintaka, J. Nishii, Y. Imaoka, J. Ohmori, S. Ura, R. Satoh, H. Nishihara, *IEEE Photonics Technol. Lett.* **2004**, *16*, 512.
[191] K. Kintaka, J. Nishii, J. Ohmori, Y. Imaoka, M. Nishihara, S. Ura, R. Satoh, H. Nishihara, *Opt. Express* **2004**, *12*, 3072.
[192] K. Hatanaka, T. Majima, K. Kintaka, J. Inoue, K. Nishio, Y. Awatsuji, S. Ura, *Electron. Lett.* **2012**, *48*, 717.
[193] M. Rumpel, M. Haefner, T. Schoder, C. Pruss, A. Voss, W. Osten, M. A. Ahmed, T. Graf, *Opt. Lett.* **2012**, *37*, 1763.
[194] C. D. Bruzewicz, J. M. Sage, J. Chiaverini, K. K. Mehta, R. J. Ram, R. McConnell, *Nat. Nanotechnol.* **2016**, *11*, 1066.
[195] K. K. Mehta, R. J. Ram, *Sci. Rep.* **2017**, *7*, 2019.
[196] W. Wang, Q. Liu, G. Zhu, X. Li, S. He, T. Sa, X. Gao, Y. Wang, *IEEE Photonics J.* **2015**, *7*, 1.
[197] Y. Chen, R. Halir, Í. Molina-Fernández, P. Cheben, J.-J. He, *Opt. Lett.* **2016**, *41*, 5059.
[198] C. J. Oton, *IEEE Photonics J.* **2016**, *8*, 1.
[199] M. Lu, H. Zhai, R. Magnusson, *Micromachines* **2011**, *2*, 150.
[200] Y. Ohtera, S. Iijima, H. Yamada, *Opt. Lett.* **2011**, *36*, 1689.
[201] Y. Ohtera, S. Iijima, H. Yamada, *Micromachines* **2012**, *3*, 101.
[202] Y. Ohtera, H. Hirose, H. Yamada, *Photonics* **2014**, *1*, 432.
[203] D. Fattal, J. Li, Z. Peng, M. Fiorentino, R. G. Beausoleil, *Nat. Photonics* **2010**, *4*, 466.
[204] L. Chrostowski, *Nat. Photonics* **2010**, *4*, 413.
[205] X. Duan, M. Zhang, Y. Huang, K. Liu, Y. Shang, X. Ren, *IEEE Photonics Technol. Lett.* **2017**, *29*, 209.
[206] G. Quaranta, G. Basset, Z. Benes, O. J. F. Martin, B. Gallinet, *J. Nanophotonics* **2018**, *12*, 016004.
[207] C. Wei, S. Liu, D. Deng, J. Shen, J. Shao, Z. Fan, *Opt. Lett.* **2006**, *31*, 1223.
[208] T. Sun, J. Ma, J. Wang, Y. Jin, H. He, J. Shao, Z. Fan, *J. Opt. Pure Appl. Opt.* **2008**, *10*, 125003.
[209] E. A. Bezus, L. L. Doskolovich, N. L. Kazanskiy, *Microelectron. Eng.* **2011**, *88*, 170.
[210] S. Somekh, A. Yariv, *Appl. Phys. Lett.* **1972**, *21*, 140.
[211] M. Neviere, P. Vincent, N. Paraire, R. Reinisch, in International Society for Optics and Photonics, **1984**, 216.
[212] P. Vincent, N. Paraire, M. Neviere, A. Koster, R. Reinisch, *JOSA B* **1985**, *2*, 1106.
[213] G. Blau, E. Popov, F. Kajzar, A. Raimond, J. F. Roux, J. L. Coutaz, *Opt. Lett.* **1995**, *20*, 1101.
[214] *Nonlinear Optics in Signal Processing* (Eds: R. W. Eason, A. Miller), Springer, Dordrecht **1993**.
[215] D. Pezzetta, C. Sibilia, M. Bertolotti, J. W. Haus, M. Scalora, M. J. Bloemer, C. M. Bowden, *JOSA B* **2001**, *18*, 1326.
[216] G. Purvinis, P. S. Priambodo, M. Pomerantz, M. Zhou, T. A. Maldonado, R. Magnusson, *Opt. Lett.* **2004**, *29*, 1108.
[217] F. Lagugné-Labarthet, F. Adamietz, V. Rodriguez, C. Sourisseau, *J. Phys. Chem. B* **2006**, *110*, 13689.
[218] M. Siltanen, S. Leivo, P. Voima, M. Kauranen, P. Karvinen, P. Vahimaa, M. Kuittinen, *Appl. Phys. Lett.* **2007**, *91*, 111109.
[219] T. Ning, H. Pietarinen, O. Hyvärinen, R. Kumar, T. Kaplas, M. Kauranen, G. Genty, *Opt. Lett.* **2012**, *37*, 4269.
[220] A. Saari, G. Genty, M. Siltanen, P. Karvinen, P. Vahimaa, M. Kuittinen, M. Kauranen, *Opt. Express* **2010**, *18*, 12298.
[221] T. Ning, O. Hyvärinen, H. Pietarinen, T. Kaplas, M. Kauranen, G. Genty, *Opt. Express* **2013**, *21*, 2012.
[222] T. Tran, V. Karagodsky, Y. Rao, W. Yang, R. Chen, C. Chase, L. C. Chuang, C. J. Chang-Hasnain, *Appl. Phys. Lett.* **2013**, *102*, 021102.
[223] J. H. Lin, C.-Y. Tseng, C.-T. Lee, J. F. Young, H.-C. Kan, C. C. Hsu, *Opt. Express* **2014**, *22*, 2790.
[224] M. H. Luong, T. T. N. Nguyen, C. T. Nguyen, I. Ledoux-Rak, N. D. Lai, *J. Phys. Appl. Phys.* **2015**, *48*, 365302.
[225] A. K. Zvezdin, V. A. Kotov, *Modern Magnetooptics and Magnetooptical Materials*, CRC Press, Boca Raton, FL **1997**.
[226] I. S. Maksymov, J. Hutomo, M. Kostylev, *Opt. Express* **2014**, *22*, 8720.
[227] S. E. Harris, *Phys. Today* **1997**, *50*, 36.
[228] S. Tibuleac, R. Magnusson, *Opt. Lett.* **2001**, *26*, 584.
[229] Y. Ding, R. Magnusson, *Opt. Lett.* **2004**, *29*, 1135.
[230] S.-G. Lee, S.-Y. Jung, H.-S. Kim, S. Lee, J.-M. Park, *Opt. Lett.* **2015**, *40*, 4241.
[231] S.-G. Lee, S.-H. Kim, K.-J. Kim, C.-S. Kee, *Appl. Phys. Lett.* **2017**, *110*, 111106.
[232] W. Lukosz, K. Tiefenthaler, presented at Second European Conference on Integrated Optics, Florence, Italy, Volume: Conf. Publication No. 227, **1983**, 152–155.
[233] K. Tiefenthaler, W. Lukosz, *Opt. Lett.* **1984**, *9*, 137.
[234] R. Magnusson, S. S. Wang, *Appl. Phys. Lett.* **1992**, *61*, 1022.
[235] D. D. Wawro, S. Tibuleac, R. Magnusson, H. Liu, in International Society for Optics and Photonics, BiOS 2000 The International Symposium on Biomedical Optics, **2000**, San Jose, CA, United States (https://doi.org/10.1117/12.384889), 86.
[236] B. T. Cunningham, P. Li, S. Schulz, B. Lin, C. Baird, J. Gerstenmaier, C. Genick, F. Wang, E. Fine, L. Laing, *J. Biomol. Screen.* **2004**, *9*, 481.
[237] S. M. O'Malley, X. Xie, A. G. Frutos, *J. Biomol. Screen.* **2007**, *12*, 117.
[238] R. Magnusson, D. Wawro, S. Zimmerman, Y. Ding, *Sensors* **2011**, *11*, 1476.
[239] A. M. Ferrie, Q. Wu, Y. Fang, *Appl. Phys. Lett.* **2010**, *97*, 223704.
[240] P. G. Hermannsson, C. Vannahme, C. L. C. Smith, A. Kristensen, *Appl. Phys. Lett.* **2014**, *105*, 071103.
[241] L. U. Kempen, R. E. Kunz, *Sens. Actuators B Chem.* **1997**, *39*, 295.
[242] P. K. Sahoo, S. Sarkar, J. Joseph, *Sci. Rep.* **2017**, *7*, 7607.
[243] M. A. Cooper, *Nat. Rev. Drug Discov.* **2002**, *1*, nrd838.
[244] Y. Fang, J. Fang, E. Tran, X. Xie, M. Hallstrom, A. G. Frutos, in *Label-Free Biosensors* (Ed: M. A. Cooper), Cambridge University Press, Cambridge **2009**, 206.
[245] J. A. Giese, J. W. Yoon, B. R. Wenner, J. W. Allen, M. S. Allen, R. Magnusson, *Opt. Lett.* **2014**, *39*, 486.

[246] B.-S. Choi, Y. Kanamori, K. Hane, *J. Opt. Pure Appl. Opt.* **2007**, *9*, 1087.
[247] D. A. Bykov, L. L. Doskolovich, V. A. Soifer, *J. Exp. Theor. Phys.* **2012**, *114*, 724.
[248] Y. Xu, X. Gao, D. Bai, G. Zhu, J. Yuan, H. Zhu, Y. Wang, *Opt. Commun.* **2017**, *387*, 89.
[249] G. L. Duveneck, M. Pawlak, D. Neuschäfer, E. Bär, W. Budach, U. Pieles, M. Ehrat, *Sens. Actuators B Chem.* **1997**, *38*, 88.
[250] S. Soria, T. Katchalski, E. Teitelbaum, A. A. Friesem, G. Marowsky, *Opt. Lett.* **2004**, *29*, 1989.
[251] S. Soria, A. Thayil. K. N., G. Badenes, M. A. Bader, A. Selle, G. Marowsky, *Appl. Phys. Lett.* **2005**, *87*, 081109.
[252] J. H. Lin, C.-Y. Tseng, C.-T. Lee, H.-C. Kan, C. C. Hsu, *Opt. Express* **2013**, *21*, 24318.
[253] A. Selle, C. Kappel, M. A. Bader, G. Marowsky, K. Winkler, U. Alexiev, *Opt. Lett.* **2005**, *30*, 1683.
[254] N. Ganesh, P. C. Mathias, W. Zhang, B. T. Cunningham, *J. Appl. Phys.* **2008**, *103*, 083104.
[255] P. Karvinen, T. Nuutinen, O. Hyvärinen, P. Vahimaa, *Opt. Express* **2008**, *16*, 16364.
[256] A. Thayil. K. N., A. Muriano, J.-P. Salvador, R. Galve, M. P. Marco, D. Zalvidea, P. Loza-Alvarez, T. Katchalski, E. Grinvald, A. A. Friesem, S. Soria, *Opt. Express* **2008**, *16*, 13315.
[257] A. Muriano, K. N. A. Thayil, J.-P. Salvador, P. Loza-Alvarez, S. Soria, R. Galve, M.-P. Marco, *Sens. Actuators B Chem.* **2012**, *174*, 394.
[258] A. Pokhriyal, M. Lu, V. Chaudhery, C.-S. Huang, S. Schulz, B. T. Cunningham, *Opt. Express* **2010**, *18*, 24793.
[259] W. Zhang, B. T. Cunningham, *Appl. Phys. Lett.* **2008**, *93*, 133115.
[260] Y. Wang, Y. Huang, J. Sun, S. Pandey, M. Lu, *Opt. Express* **2015**, *23*, 28567.
[261] Y.-C. Lee, C.-F. Huang, J.-Y. Chang, M.-L. Wu, *Opt. Express* **2008**, *16*, 7969.
[262] T. Khaleque, R. Magnusson, *J. Nanophotonics* **2014**, *8*, 083995.
[263] M. Kroll, S. Fahr, C. Helgert, C. Rockstuhl, F. Lederer, T. Pertsch, *Phys. Status Solidi A* **2008**, *205*, 2777.
[264] D. Duché, L. Escoubas, J.-J. Simon, P. Torchio, W. Vervisch, F. Flory, *Appl. Phys. Lett.* **2008**, *92*, 193310.
[265] D.-H. Ko, J. R. Tumbleston, L. Zhang, S. Williams, J. M. DeSimone, R. Lopez, E. T. Samulski, *Nano Lett.* **2009**, *9*, 2742.
[266] G. Gomard, E. Drouard, X. Letartre, X. Meng, A. Kaminski, A. Fave, M. Lemiti, E. Garcia-Caurel, C. Seassal, *J. Appl. Phys.* **2010**, *108*, 123102.
[267] W. Wu, R. Magnusson, *Opt. Lett.* **2012**, *37*, 2103.
[268] M. S. Badar, M. R. Saleem, *Opt. Int. J. Light Electron Opt.* **2017**, *128*, 50.
[269] U. W. Paetzold, S. Lehnen, K. Bittkau, U. Rau, R. Carius, *Nano Lett.* **2014**, *14*, 6599.
[270] Y. D. Chong, L. Ge, H. Cao, A. D. Stone, *Phys. Rev. Lett.* **2010**, *105*, 053901.
[271] A. L. Fannin, J. W. Yoon, B. R. Wenner, J. W. Allen, M. S. Allen, R. Magnusson, *IEEE Photonics J.* **2016**, *8*, 1.
[272] A. Y. Zhu, S. Zhu, G.-Q. Lo, *Opt. Express* **2014**, *22*, 2247.
[273] X. Zhang, Y. Huang, X. Ren, H. Huang, Q. Wang, *Appl. Opt.* **2009**, *48*, 6760.
[274] I. R. McKerracher, L. Fu, H. H. Tan, C. Jagadish, *J. Phys. Appl. Phys.* **2013**, *46*, 095104.
[275] M. Verdun, B. Portier, K. Jaworowicz, J. Jaeck, F. Lelarge, S. Guilet, C. Dupuis, R. Haïdar, F. Pardo, J.-L. Pelouard, *Appl. Phys. Lett.* **2016**, *108*, 053501.
[276] Z. Ruan, L. Shen, S. Zheng, J. Wang, *Opt. Express* **2017**, *25*, 18250.
[277] N. Destouches, D. Blanc, J. Franc, S. Tonchev, N. Hendrickx, P. V. Daele, O. Parriaux, *Opt. Express* **2007**, *15*, 16870.
[278] D. A. Bykov, L. L. Doskolovich, V. A. Soifer, *Opt. Lett.* **2011**, *36*, 3509.
[279] L. L. Doskolovich, E. A. Bezus, N. V. Golovastikov, D. A. Bykov, V. A. Soifer, *Opt. Express* **2017**, *25*, 22328.
[280] S. V. Emelyanov, D. A. Bykov, N. V. Golovastikov, L. L. Doskolovich, V. A. Soifer, *Dokl. Phys.* **2016**, *61*, 108.
[281] D. A. Bykov, L. L. Doskolovich, V. A. Soifer, *JOSA A* **2012**, *29*, 1734.
[282] D. A. Bykov, L. L. Doskolovich, N. V. Golovastikov, V. A. Soifer, *J. Opt.* **2013**, *15*, 105703.
[283] N. V. Golovastikov, D. A. Bykov, L. L. Doskolovich, V. A. Soifer, *J. Exp. Theor. Phys.* **2015**, *121*, 785.
[284] N. Savage, *IEEE Spectr.* **2002**, *39*, 32.
[285] M. Niraula, J. W. Yoon, R. Magnusson, *Opt. Lett.* **2015**, *40*, 5062.
[286] S. Ura, T. Asada, S. Yamaguchi, K. Nishio, A. Horii, K. Kintaka, *Opt. Express* **2006**, *14*, 7057.
[287] S. Ura, M. Hamada, J. Ohmori, K. Nishio, K. Kintaka, *Appl. Opt.* **2006**, *45*, 22.
[288] K. Kintaka, K. Shimizu, Y. Kita, S. Kawanami, J. Inoue, S. Ura, J. Nishii, *Opt. Express* **2010**, *18*, 25108.
[289] K. Kintaka, Y. Kita, K. Shimizu, H. Matsuoka, S. Ura, J. Nishii, *Opt. Lett.* **2010**, *35*, 1989.
[290] D. R. Mason, S. J. Goodman, D. K. Gramotnev, T. A. Nieminen, *Appl. Opt.* **2006**, *45*, 1804.
[291] R. Magnusson, *Opt. Lett.* **2012**, *37*, 3792.
[292] M. Streshinsky, R. Shi, A. Novack, R. T. P. Cher, A. E.-J. Lim, P. G.-Q. Lo, T. Baehr-Jones, M. Hochberg, *Opt. Express* **2013**, *21*, 31019.
[293] T. Sang, G. Chen, Y. Wang, B. Wang, W. Jiang, T. Zhao, S. Cai, *Opt. Laser Technol.* **2016**, *83*, 163.
[294] H. Tamada, T. Doumuki, T. Yamaguchi, S. Matsumoto, *Opt. Lett.* **1997**, *22*, 419.
[295] R. Magnusson, M. Shokooh-Saremi, *Opt. Express* **2008**, *16*, 3456.
[296] K. J. Lee, R. LaComb, B. Britton, M. Shokooh-Saremi, H. Silva, E. Donkor, Y. Ding, R. Magnusson, *IEEE Photonics Technol. Lett.* **2008**, *20*, 1857.
[297] K. Lee, J. Curzan, M. Shokooh-Saremi, R. Magnusson, in *Frontiers in Optics 2011*,Optical Society of America **2011**, FWU2.
[298] K. J. Lee, J. Curzan, M. Shokooh-Saremi, R. Magnusson, *Appl. Phys. Lett.* **2011**, *98*, 211112.
[299] K. J. Lee, J. Giese, L. Ajayi, R. Magnusson, E. Johnson, *Opt. Express* **2014**, *22*, 9271.
[300] Y. Jourlin, S. Tonchev, A. V. Tishchenko, F. Lacour, O. Parriaux, *Opt. Express* **2012**, *20*, 29155.
[301] J. W. Yoon, K. J. Lee, R. Magnusson, *Opt. Express* **2015**, *23*, 28849.
[302] I. Vartiainen, J. Tervo, M. Kuittinen, *Opt. Lett.* **2009**, *34*, 1648.
[303] I. Vartiainen, T. Saastamoinen, J. Tervo, M. Kuittinen, *Opt. Lett.* **2012**, *37*, 314.
[304] V. A. Sychugov, A. V. Tishchenko, *Sov. J. Quantum Electron.* **1981**, *11*, 421.
[305] R. Magnusson, M. Shokooh-Saremi, E. G. Johnson, *Opt. Lett.* **2010**, *35*, 2472.
[306] K. Chaganti, I. Salakhutdinov, I. Avrutsky, G. W. Auner, *Opt. Express* **2006**, *14*, 4064.
[307] I. Avrutsky, K. Chaganti, I. Salakhutdinov, G. Auner, *Appl. Opt.* **2006**, *45*, 7811.
[308] M. Ramuz, L. Bürgi, R. Stanley, C. Winnewisser, *J. Appl. Phys.* **2009**, *105*, 084508.
[309] M. Ramuz, D. Leuenberger, L. Bürgi, *J. Polym. Sci. Part B Polym. Phys.* **2010**, *49*, 80.
[310] N. Ganesh, A. Xiang, N. B. Beltran, D. W. Dobbs, B. T. Cunningham, *Appl. Phys. Lett.* **2007**, *90*, 081103.
[311] H.-A. Lin, C.-S. Huang, *IEEE Photonics Technol. Lett.* **2016**, *1*, 1042.
[312] H.-A. Lin, H.-Y. Hsu, C.-W. Chang, C.-S. Huang, *Opt. Express* **2016**, *24*, 10972.
[313] R. Bhargava, *Appl. Spectrosc.* **2012**, *66*, 1091.
[314] A. K. Kodali, M. Schulmerich, J. Ip, G. Yen, B. T. Cunningham, R. Bhargava, *Anal. Chem.* **2010**, *82*, 5697.

[315] J.-N. Liu, M. V. Schulmerich, R. Bhargava, B. T. Cunningham, *Opt. Express* **2011**, *19*, 24182.
[316] D. Gallegos, K. D. Long, H. Yu, P. P. Clark, Y. Lin, S. George, P. Nath, B. T. Cunningham, *Lab. Chip* **2013**, *13*, 2124.
[317] Y. Horie, A. Arbabi, S. Han, A. Faraon, *Opt. Express* **2015**, *23*, 29848.
[318] O. Solgaard, *Appl. Opt.* **2010**, *49*, F18.
[319] R. Magnusson, Y. Ding, *IEEE Photonics Technol. Lett.* **2006**, *18*, 1479.
[320] T. Sang, T. Cai, S. Cai, Z. Wang, *J. Opt.* **2011**, *13*, 125706.
[321] R. Magnusson, M. Shokooh-Saremi, *Opt. Express* **2007**, *15*, 10903.
[322] R. Magnusson, M. Shokooh-Saremi, presented at 2008 IEEE Aerosp. Conf., Big Sky, Montana **2008**, 1.
[323] Y. Kanamori, N. Matsuyama, K. Hane, *IEEE Photonics Technol. Lett.* **2008**, *20*, 1136.
[324] H. Honma, K. Takahashi, M. Ishida, K. Sawada, *Jpn. J. Appl. Phys.* **2012**, *51*, 11PA01.
[325] A. Sharon, D. Rosenblatt, A. A. Friesem, H. G. Weber, H. Engel, R. Steingrueber, *Opt. Lett.* **1996**, *21*, 1564.
[326] N. Dudovich, G. Levy-Yurista, A. Sharon, A. A. Friesem, H. G. Weber, *IEEE J. Quantum Electron.* **2001**, *37*, 1030.
[327] H. Ichikawa, H. Kikuta, *JOSA A* **2005**, *22*, 1311.
[328] K. Y. Lee, J. W. Yoon, S. H. Song, R. Magnusson, *Sci. Rep.* **2017**, *7*, 46508.
[329] F. Yang, G. Yen, G. Rasigade, J. A. N. T. Soares, B. T. Cunningham, *Appl. Phys. Lett.* **2008**, *92*, 091115.
[330] C.-T. Wang, H.-H. Hou, P.-C. Chang, C.-C. Li, H.-C. Jau, Y.-J. Hung, T.-H. Lin, *Opt. Express* **2016**, *24*, 22892.
[331] A. S. P. Chang, K. J. Morton, H. Tan, P. F. Murphy, W. Wu, S. Y. Chou, *IEEE Photonics Technol. Lett.* **2007**, *19*, 1457.
[332] L. Qian, D. Zhang, B. Dai, Y. Huang, C. Tao, R. Hong, S. Zhuang, *Opt. Lett.* **2015**, *40*, 713.
[333] L. Qian, D. Zhang, B. Dai, Q. Wang, Y. Huang, S. Zhuang, *Opt. Express* **2015**, *23*, 18300.
[334] C.-T. Wang, P.-C. Chang, J. J. Lin, M. C. Tai, Y.-J. Hung, T.-H. Lin, *Appl. Opt.* **2017**, *56*, 4219.
[335] D. C. Zografopoulos, E. E. Kriezis, R. Beccherelli, *IEEE Photonics Technol. Lett.* **2017**, *29*, 1367.
[336] S. Block, E. Gamet, F. Pigeon, *IEEE J. Quantum Electron.* **2005**, *41*, 1049.
[337] M. J. Uddin, R. Magnusson, *IEEE Photonics Technol. Lett.* **2013**, *25*, 1412.
[338] A. N. Enemuo, R. R. Chaudhuri, Y. Song, S. W. Seo, *IEEE Sens. J.* **2015**, *15*, 4213.
[339] S. Giet, C.-L. Lee, S. Calvez, M. D. Dawson, N. Destouches, J.-C. Pommier, O. Parriaux, *Opt. Express* **2007**, *15*, 16520.
[340] A. Aubourg, M. Rumpel, J. Didierjean, N. Aubry, T. Graf, F. Balembois, P. Georges, M. A. Ahmed, *Opt. Lett.* **2014**, *39*, 466.
[341] M. M. Vogel, M. Rumpel, B. Weichelt, A. Voss, M. Haefner, C. Pruss, W. Osten, M. A. Ahmed, T. Graf, *Opt. Express* **2012**, *20*, 4024.
[342] F. Brückner, D. Friedrich, T. Clausnitzer, O. Burmeister, M. Britzger, E.-B. Kley, K. Danzmann, A. Tünnermann, R. Schnabel, *Opt. Express* **2009**, *17*, 163.
[343] M. Punturo, H. Lück, M. Beker, *Advanced Interferometers and the Search for Gravitational Waves*, Springer, Cham **2014**, p. 333.
[344] N. Mavalvala, D. E. McClelland, G. Mueller, D. H. Reitze, R. Schnabel, B. Willke, *Gen. Relativ. Gravit.* **2011**, *43*, 569.
[345] D. Friedrich, B. W. Barr, F. Brückner, S. Hild, J. Nelson, J. Macarthur, M. V. Plissi, M. P. Edgar, S. H. Huttner, B. Sorazu, S. Kroker, M. Britzger, E.-B. Kley, K. Danzmann, A. Tünnermann, K. A. Strain, R. Schnabel, *Opt. Express* **2011**, *19*, 14955.
[346] F. Brückner, D. Friedrich, T. Clausnitzer, M. Britzger, O. Burmeister, K. Danzmann, E.-B. Kley, A. Tünnermann, R. Schnabel, *Phys. Rev. Lett.* **2010**, *104*, 163903.
[347] N. Destouches, J.-C. Pommier, O. Parriaux, T. Clausnitzer, N. Lyndin, S. Tonchev, *Opt. Express* **2006**, *14*, 12613.
[348] F. Bencheikh, A. S. D. Sandanayaka, T. Matsushima, J. C. Ribierre, C. Adachi, *J. Appl. Phys.* **2017**, *121*, 233107.
[349] X. Buet, E. Daran, D. Belharet, F. Lozes-Dupuy, A. Monmayrant, O. Gauthier-Lafaye, *Opt. Express* **2012**, *20*, 9322.
[350] N. Rassem, A.-L. Fehrembach, E. Popov, *JOSA A* **2015**, *32*, 420.
[351] S. Ura, S. Murata, Y. Awatsuji, K. Kintaka, *Opt. Express* **2008**, *16*, 12207.
[352] K. Kintaka, T. Majima, J. Inoue, K. Hatanaka, J. Nishii, S. Ura, *Opt. Express* **2012**, *20*, 1444.
[353] J. Inoue, T. Majima, K. Hatanaka, K. Kintaka, K. Nishio, Y. Awatsuji, S. Ura, *Appl. Phys. Express* **2012**, *5*, 022201.
[354] K. Kintaka, K. Asai, K. Yamada, J. Inoue, S. Ura, *IEEE Photonics Technol. Lett.* **2017**, *29*, 201.
[355] J. Inoue, T. Kondo, K. Kintaka, K. Nishio, S. Ura, *Opt. Express* **2015**, *23*, 3020.
[356] J. Inoue, H. Okuda, K. Kintaka, K. Nishio, S. Ura, *Jpn. J. Appl. Phys.* **2017**, *56*, 072001.
[357] C. Sciancalepore, B. B. Bakir, X. Letartre, J.-M. Fedeli, N. Olivier, D. Bordel, C. Seassal, P. Rojo-Romeo, P. Regreny, P. Viktorovitch, *J. Light. Technol.* **2011**, *29*, 2015.
[358] C. Sciancalepore, B. B. Bakir, X. Letartre, J. Harduin, N. Olivier, C. Seassal, J. M. Fedeli, P. Viktorovitch, *IEEE Photonics Technol. Lett.* **2012**, *24*, 455.
[359] K. Kintaka, K. Hatanaka, J. Inoue, S. Ura, *Appl. Phys. Express* **2013**, *6*, 102203.
[360] K. Kintaka, T. Majima, K. Hatanaka, J. Inoue, S. Ura, *Opt. Lett.* **2012**, *37*, 3264.
[361] J. Inoue, T. Ogura, T. Kondo, K. Kintaka, K. Nishio, Y. Awatsuji, S. Ura, *Opt. Lett.* **2014**, *39*, 1893.
[362] R. Laberdesque, O. Gauthier-Lafaye, H. Camon, A. Monmayrant, M. Petit, O. Demichel, B. Cluzel, *JOSA A* **2015**, *32*, 1973.
[363] N. Rassem, E. Popov, A.-L. Fehrembach, *Opt. Quantum Electron.* **2015**, *47*, 3171.
[364] P. C. Chaumet, A. Sentenac, A.-L. Fehrembach, *Opt. Quantum Electron.* **2017**, *49*, 71.
[365] M. J. Byrd, R. H. Woodward, A. J. Pung, E. G. Johnson, K. J. Lee, R. Magnusson, P. Binun, K. McCormick, *IEEE Photonics Technol. Lett.* **2014**, *26*, 2311.
[366] I. A. Avrutskiĭ, V. P. Duraev, E. T. Nedelin, A. M. Prokhorov, A. S. Svakhin, V. A. Sychugov, A. V. Tishchenko, *Sov. J. Quantum Electron.* **1988**, *18*, 362.
[367] I. Avrutsky, R. Rabady, *Opt. Lett.* **2001**, *26*, 989.
[368] K. Yamada, K. Asai, Y. H. Ko, K. Kintaka, K. J. Lee, J. Inoue, S. Ura, R. Magnusson, *Appl. Phys. Express* **2016**, *9*, 122501.
[369] R. A. Sims, Z. A. Roth, C. C. C. Willis, P. Kadwani, T. S. McComb, L. Shah, V. Sudesh, M. Poutous, E. G. Johnson, M. Richardson, *Opt. Lett.* **2011**, *36*, 737.
[370] P. Srinivasan, M. K. Poutous, Z. A. Roth, Y. O. Yilmaz, R. C. Rumpf, E. G. Johnson, *Opt. Express* **2009**, *17*, 20365.
[371] M. Byrd, A. Pung, E. Johnson, K. Lee, R. Magnusson, P. Binun, K. McCormick, *IEEE Photonics Technol. Lett.* **2015**, *27*, 2166.
[372] T. Kondo, S. Ura, R. Magnusson, *JOSA A* **2015**, *32*, 1454.
[373] A. A. Mehta, R. C. Rumpf, Z. A. Roth, E. G. Johnson, *IEEE Photonics Technol. Lett.* **2007**, *19*, 2030.
[374] Y. Li, I. R. Srimathi, R. H. Woodward, A. J. Pung, M. K. Poutous, R. K. Shori, E. G. Johnson, *IEEE Photonics Technol. Lett.* **2012**, *24*, 2300.
[375] R. L. Renesse, *Optical Document Security*, 3rd ed., Artech House, Boston, MA **2004**.
[376] K. H. Knop, *US4426130A*, **1984**.
[377] M.-L. Wu, C.-L. Hsu, H.-C. Lan, H.-I. Huang, Y.-C. Liu, Z.-R. Tu, C.-C. Lee, J.-S. Lin, C.-C. Su, J.-Y. Chang, *Opt. Lett.* **2007**, *32*, 1614.
[378] SURYS DID™, http://surys.com (accessed: July **2017**).

[379] SURYS for DID™ Graphic Wave, http://surys.com (accessed: July **2017**).
[380] I. Evenor, E. Grinvald, F. Lenz, S. Levit, *Eur. Phys. J. D* **2012**, *66*, 231.
[381] L. Su, R. Trivedi, N. V. Sapra, A. Y. Piggott, D. Vercruysse, J. Vučković, *Opt. Express* **2018**, *26*, 4023.
[382] D. Lin, M. Melli, E. Poliakov, P. S. Hilaire, S. Dhuey, C. Peroz, S. Cabrini, M. Brongersma, M. Klug, *Sci. Rep.* **2017**, *7*, 2286.
[383] S. Fan, J. D. Joannopoulos, *Phys. Rev. B* **2002**, *65*, 235112.
[384] W. Wang, A. Klots, Y. Yang, W. Li, I. I. Kravchenko, D. P. Briggs, K. I. Bolotin, J. Valentine, *Appl. Phys. Lett.* **2015**, *106*, 181104.
[385] T. Matsui, H. Iizuka, *J. Opt.* **2017**, *19*, 03LT01.
[386] Q. Guo, C. Li, B. Deng, S. Yuan, F. Guinea, F. Xia, *ACS Photonics* **2017**, *4*, 2989.